Inorganic Chemistry

Article

pubs.acs.org/IC

Facile Metalation of Hbzq by [*cis*-Pt(C_6F_5)$_2$(thf)$_2$]: A Route to a Pentafluorophenyl Benzoquinolate Solvate Complex That Easily Coordinates Terminal Alkynes. Spectroscopic and Optical Properties†

Jesús R. Berenguer, Elena Lalinde,* M. Teresa Moreno, Sergio Sánchez, and Javier Torroba

Departamento de Química—Grupo de Síntesis Química de La Rioja, UA-CSIC, Universidad de La Rioja, 26006 Logroño, Spain

Supporting Information

ABSTRACT: A new neutral cyclometalated platinum(II) solvate complex [*cis*-Pt(bzq)(C_6F_5)(acetone)] (**1**) has been prepared by easy C−H activation of 7,8-benzo[*h*]quinoline on the coordination sphere of [*cis*-Pt(C_6F_5)$_2$(thf)$_2$] (thf = tetrahydrofuran). The study of the reaction pathway has led us to the preparation of the bis(Hbzq) product [*cis*-Pt(C_6F_5)$_2$(Hbzq)$_2$] (**2**) and the benzoquinoline−benzoquinolate derivative [Pt(bzq)(C_6F_5)(Hbzq)] (**3**). This latter complex has been characterized by X-ray diffraction, showing the occurrence of $\pi\cdots\pi$ intermolecular stacking interactions associated to the deprotonated bzq units. The acetone molecule in [*cis*-Pt(bzq)(C_6F_5)(acetone)] can be easily displaced by alkynes, allowing the synthesis of the first reported η^2-alkyne-cycloplatinate complexes [Pt(bzq)(C_6F_5)(η^2-RC≡CR′)] (R = H, R′ = Ph **4**, ^{t}Bu **5**, Fc **6**; R = R′ = Ph **7**), which have been fully characterized spectroscopically and by DFT studies. These alkyne complexes are only moderately stable in solution, and all attempts to obtain crystals suitable for X-ray diffraction were fruitless. Nevertheless, in the case of the ferrocenyl derivative, crystals of complex [Pt(κN:η^2-bzq-C≡CFc)(C_6F_5)(μ-κC^{α}:η^2-C≡CFc)Pt(bzq)(C_6F_5)] (**8**), containing an unusual alkynyl-functionalized benzoquinoline chelate ligand, were systematically obtained. All complexes (except those containing the ferrocenyl fragment) present emissive properties in solution and solid state (77 K), related, in general, with intraligand (bzq) excited states with some mixing ^{3}MLCT character, as supported by theoretical calculations. In solid state at room temperature, aggregation induced emission (AIE) is observed likely generated by intermolecular $\pi\cdots\pi$ stacking, as supporting by DFT calculations on $\mathbf{3}_2$. Interestingly, both types of excited states (^{3}IL/^{3}MLCT and AIE) seem to be close in energy in complexes **1** and **3**, which show a significant luminescent thermochromism (green 77 K to orange 298 K).

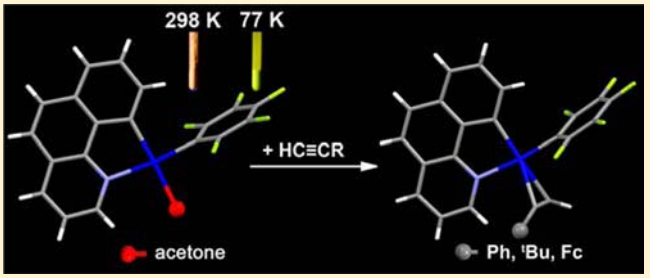

INTRODUCTION

The search for new emitting coordination complexes is currently attracting widespread interest from both the standpoint of fundamental properties and their potential in the development of optoelectronic devices.[1] In this area, a significant effort has focused on the design and synthesis of square-planar platinum(II) complexes containing alkynyl, polypyridyl, and/or cyclometalating ligands, due to their rich and readily tunable photophysical properties, as well as their tendency to form metal−metal and π−π stacking interactions. Several recent reviews cover different aspects of these complexes, including the nature of their excited states and the wide variety of promising applications.[2] In particular, cyclometalating (C^N, N^C^N, C^N^N, C^N^C) platinum complexes have shown potential in highly efficient organic light-emitting diode (OLED) devices,[2,3] as luminescent molecular sensors and in biological labeling[2,4] and photocatalysis.[5] For these complexes the photophysical properties are usually determined by the nature and the degree of conjugation of the cyclometalating ligand.[2,6] In general, the strong field nature of the cyclometalating ligand pushes the undesired nonradiative metal centered (d−d) excited states to higher energies, thus favoring phosphorescence from a variety of lowest triplet excited states, including ligand centered (LC), charge transfer (MLCT, LL′CT), or metal-metal-to-ligand charge transfer (MMLCT) excited states. The coligands may have also a remarkable effect on the characteristics of the lowest excited state, and to date, the most common auxiliary ligands used are β-diketonates (O^O),[7] phosphines, and related strong field ligands such as alkynyl (C≡CR$^-$), CO, C≡NR, and CN$^-$.[2,8]

On the other hand, alkyl and aryl heteroleptic platinum(II) complexes with cyclometalating (C^N) ligands have also attracted the attention of many chemists.[9] The synthesis of these complexes often requires selective intramolecular C−X (X = H, halide) bond activation, and on many occasions, they are involved in C−C bond coupling processes, which are among the most pursued goals in transition metal chemistry.[9,10] The interest in these systems has mainly focused on synthetic strategies and mechanistic aspects, and little is known about their optical properties.[9k,l] In our continued efforts to design

Received: July 18, 2012
Published: October 18, 2012

dx.doi.org/10.1021/ic301563u | *Inorg. Chem.* 2012, 51, 11665−11679

Scheme 1

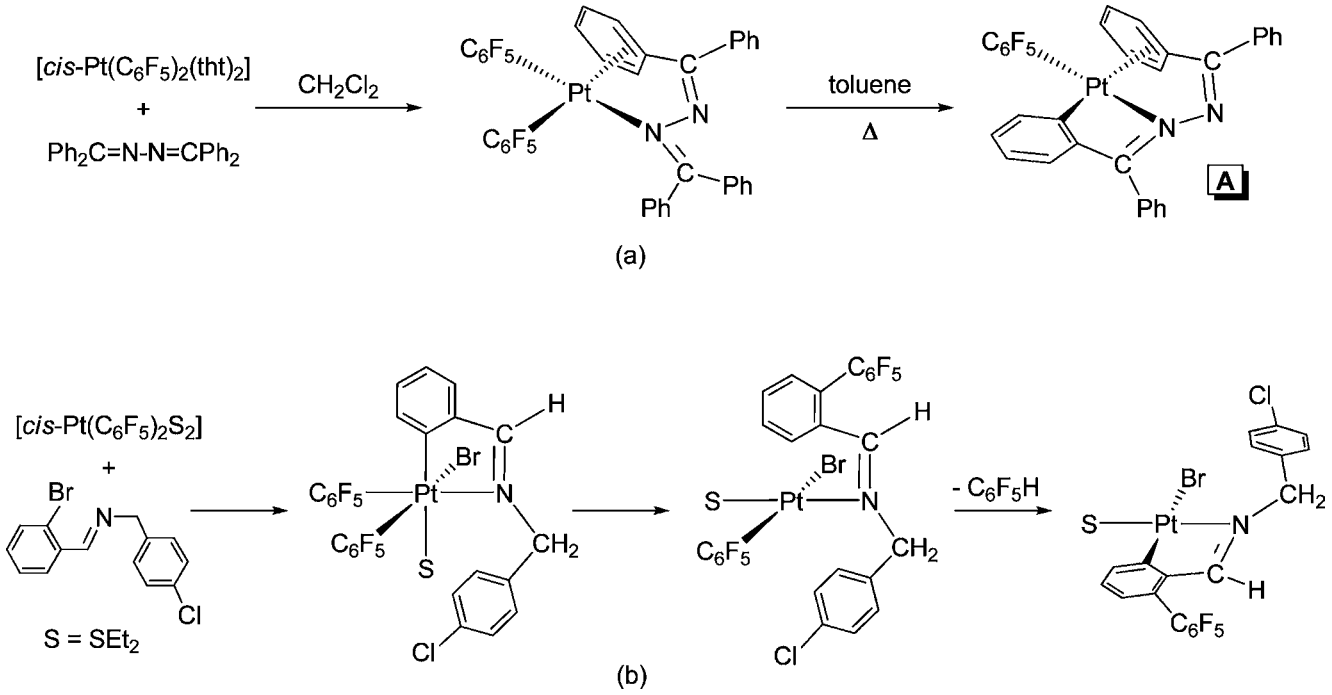

homo- and heteropolynuclear luminescent benzoquinolate platinum(II) complexes, Forniés and Lalinde et al. previously reported the anionic derivative $(NBu_4)[Pt(bzq)(C_6F_5)_2]$, which has been shown to be not only an efficient green emitter,[11] but also an excellent precursor to polymetallic species stabilized by Pt→M donor bonds and in some cases η^1-C(bzq)···M bonding interactions.[11,12] In this contribution, we report on the synthesis of two neutral pentafluorophenyl benzoquinolate complexes $[Pt(bzq)(C_6F_5)L]$ (L = acetone **1**, Hbzq **3**), which are related to the N,N coordinated complex $[cis\text{-}Pt(C_6F_5)_2(Hbzq)_2]$, **2**, as well as on their photophysical properties. We also sought to probe the feasibility of the substitution of the acetone solvent in complex **1** for alkynes. The rationale of our choice mainly rests on the knowledge that Pt(II)-alkynes, in particular with terminal alkynes, are very rare,[13] and to the best of our knowledge, there is no report on terminal alkynes coordinated to a cycloplatinated fragment.[14] Here we wish to report on the synthesis, characterization, and optical properties of the η^2-alkyne complexes $[Pt(bzq)(C_6F_5)(HC{\equiv}CR)]$ (R = Ph **4**, ^{t}Bu **5**, Fc **6**) and $[Pt(bzq)(C_6F_5)(PhC{\equiv}CPh)]$, **7**, as well as on the unusual formation of the diplatinum complex $[Pt(\kappa N{:}\eta^2\text{-bzq-}C{\equiv}CFc)(C_6F_5)(\mu\text{-}\kappa C^{\alpha}{:}\eta^2\text{-}C{\equiv}CFc)Pt(bzq)(C_6F_5)]$, **8**, containing a rare functionalized akynyl-benzoquinoline (bzq-C≡CFc)-10 as a chelating $\kappa N{:}\eta^2$-C≡C ligand.

RESULT AND DISCUSSION

Preparation and Characterization of Complexes 1−3. Efficient cyclometalation promoted by transition metal complexes remains one of the most challenging fields in modern chemistry, because of its many successful applications in organic synthesis.[10,15] In this area, since the first report of a platinum(II) complex containing a N^C orthometalated ligand,[16] the study of this kind of cycloplatinated system has experienced continuous growing, giving rise not only to a wide range of interesting complexes, but also to many mechanistic details of the C−H bond activation in cyclometalation.[10,15] Among the variety of platinum substrates, common starting materials for cycloplatination are species containing labile ligands, $[cis\text{-}PtX_2S_2]$ (X = Cl, R; S = SMe_2, NCMe, dmso, and so forth), and dimeric complexes, $[PtR_2(\mu\text{-}SMe_2)]_2$ (R = Me, Aryl), because they enable the required initial N-coordination of the HC^N ligand. By using these precursors, a number of neutral alkyl and aryl cycloplatinate complexes [Pt(C^N)RS] (S = labile solvent)[9] and very interesting series of rollover N′(3) mono- and polynuclear platinum complexes,[9d,e,17] generated by unusual cyclometalation of 6-substituted, and unsubstituted 2,2′-bypiridyne ligands, have been reported. On the contrary, and probably due to the higher thermal stability of perfluoro organyl R^F-platinum bonds, reports related to the cyclometalation of potential N-ligands by $[cis\text{-}PtR^F{}_2S_2]$ are very rare.[9b,18] The first example was published by Professor Forniés in 1992, who reported (Scheme 1a) the synthesis of complex $[Pt(C_6F_5)(C_6H_4C(Ph){=}N{-}N{=}CPh_2)]$, **A**, containing the deprotonated benzophenone azine acting as tridentate $\kappa^2C,N\text{-}\eta^2$(phenyl) ligand.[18] More recently, Crespo and Martínez et al. have found that the reaction of $[cis\text{-}Pt(C_6F_5)_2S_2]$ (S = SEt_2, SMe_2) with the imine $2\text{-}BrC_6H_4CH{=}NCH_2(4'\text{-}ClC_6H_4)$ (Scheme 1b) evolves with final formation of Pt(II) metalated complexes $[PtBr\{6\text{-}(C_6F_5)(2\text{-}C)C_5H_3CHN\text{-}CH_2(4'\text{-}ClC_6H_4)\}\text{-}S]$, containing a biaryl linkage involving one of the C_6F_5 groups.[9b] In this context and aiming to obtain a solvate monopentafluorophenylbenzoquinolate complex, we decide to investigate the reactivity of $[cis\text{-}Pt(C_6F_5)_2(thf)_2]$ (thf = tetrahydrofuran) toward 7,8-benzo[*h*]quinoline.

As is shown in eq 1, the reaction of $[cis\text{-}Pt(C_6F_5)_2(thf)_2]$ with 1 equiv of 7,8-benzoquinoline in refluxing acetone for 2.5 h renders the benzoquinolate complex **1** in almost quantitative yield (97%). The structure of complex **1** was based on spectroscopic data (^{1}H, ^{19}F, ^{13}C{^{1}H}), mass spectrometry, and elemental analysis. In particular, the very high value of the $^{195}Pt{-}F_{ortho}$ coupling constant (501 Hz) found in the ^{19}F NMR spectrum is consistent with the N atom in *trans* position to the C_{ipso} atom of the C_6F_5 group. The selective formation of this

dx.doi.org/10.1021/ic301563u | Inorg. Chem. 2012, 51, 11665−11679

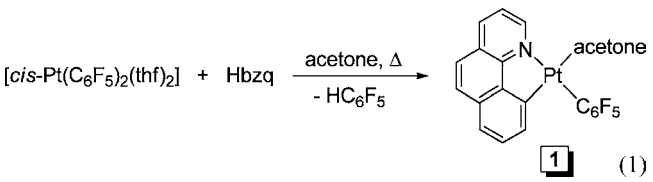

(1)

geometric isomer is coherent with the well-known *transphobia* effect,[8e,19] which places the ligand of lower *trans* influence (acetone solvent) *trans* to the metalated C^{10} atom. The complete ^{1}H and ^{13}C assignment of the deprotonated bzq ligand was performed on the basis of 2D-NMR experiments ($^{1}H-^{1}H$ COSY, $^{1}H-^{13}C$ HSQC and HMBC; see Figure S1 in Supporting Information). Thus, the H^{9} proton is observed, flanked by Pt satellites, relatively upfield (δ 6.90) on account of the expected anisotropic effect of the C_6F_5 ring. The very high ^{195}Pt coupling constant for this H^{9} proton ($^{3}J_{Pt-H}$ = 70 Hz) is also consistent with the CH_3COCH_3 coordinated (δ_H 2.06; δ_C 31.6 and 206.8) *trans* to the C^{10}-metalated carbon atom (δ 142.8). For previously studied reactions between [*cis*-Pt$(Ar)_2S_2$] (Ar = $C_6H_3Me_2$-3,5; $C_6H_3(CF_3)_2$-3,5; Ph; S = dmso, NCMe) and 2-arylpyridine ligands (HPhpy, HCF_3Phpy), it has been shown that the reaction involves the formation of intermediate complexes [*cis*-Pt$(Ar)_2$(HPhpy)S] having a monodentate HPhpy ligand (detected by NMR spectroscopy and characterized by X-ray for complex [*cis*-Pt$(C_6H_3Me_2$-3,5$)_2$(HPhCF$_3$py)(dmso)][9a]). The final monoaryl cycloplatinated complexes were suggested to be formed from this intermediate by intramolecular oxidative addition of the C−H to the Pt(II), followed by arene reductive elimination. To get more insight in the reaction pathway leading to complex **1**, the reaction was monitored by ^{1}H and ^{19}F NMR spectroscopy in acetone-d_6. Interestingly, when 1 equiv of Hbzq is added to [*cis*-Pt$(C_6F_5)_2$(thf)$_2$] at room temperature, a clean equimolar mixture of the solvate precursor and the bis(Hbzq) coordination product [*cis*-Pt$(C_6F_5)_2$(Hbzq)$_2$], **2**, was formed (Scheme 2). The mixture converts slowly and almost quantitatively (~2 h) into the cyclometalated derivative **1** with formal elimination of C_6F_5H, as observed by ^{19}F NMR spectroscopy. No other intermediate was detected. The formation of the saturated complex **2** is likely related to the presence of very weakly coordinating tetrahydrofuran molecules in the precursor, which facilitates the disubstitution and formation of two relatively strong Pt−N bonds, making **2** thermodynamically more stable than the monosubstitution complex [*cis*-Pt$(C_6F_5)_2$(Hbzq)S]. Similar saturated and stable coordination palladium complexes of type [M(E−CR)$_2X_n$] have been detected and isolated in cyclometalation processes.[20] Probably, the excessive crowding around platinum in complex **2** facilitates the transient decoordination of one of the Hbzq ligands, yielding the coordinatively unsaturated 14 electron complex **2′** as the key intermediate. The final C−H bond activation in **2′** could be facilitated by the fact that the rigid 7,8-benzo[*h*]quinoline is expected to be roughly perpendicular to the coordination plane, allowing the $C^{10'}-H$ vector to be close to the Pt center (Scheme 2).[21]

In order to confirm that complex **2** is an adequate precursor for the preparation of **1**, it was independently generated, as a yellow solid, by reaction of [*cis*-Pt$(C_6F_5)_2$(thf)$_2$] with 2 equiv of Hbzq (Scheme 3i). Although its formation is immediate and quantitative, the synthesis and characterization of **2** must be carried out at low temperature (see Experimental Section), because it is unstable in solution, evolving even at low temperature to the new cyclometalated complex [Pt(bzq)(C_6F_5)(Hbzq)], **3** (Scheme 3ii). Complex **2** was found to react, even at room temperature, with 1 equiv of the solvate [*cis*-Pt$(C_6F_5)_2$(thf)$_2$] in acetone yielding **1** (Scheme 3iii), and as was expected, the acetone molecule in **1** can be replaced by Hbzq to directly give **3** in very high yield (75%, Scheme 3iv). Despite of many efforts to crystallize these **1**−**3** complexes, we

Scheme 2

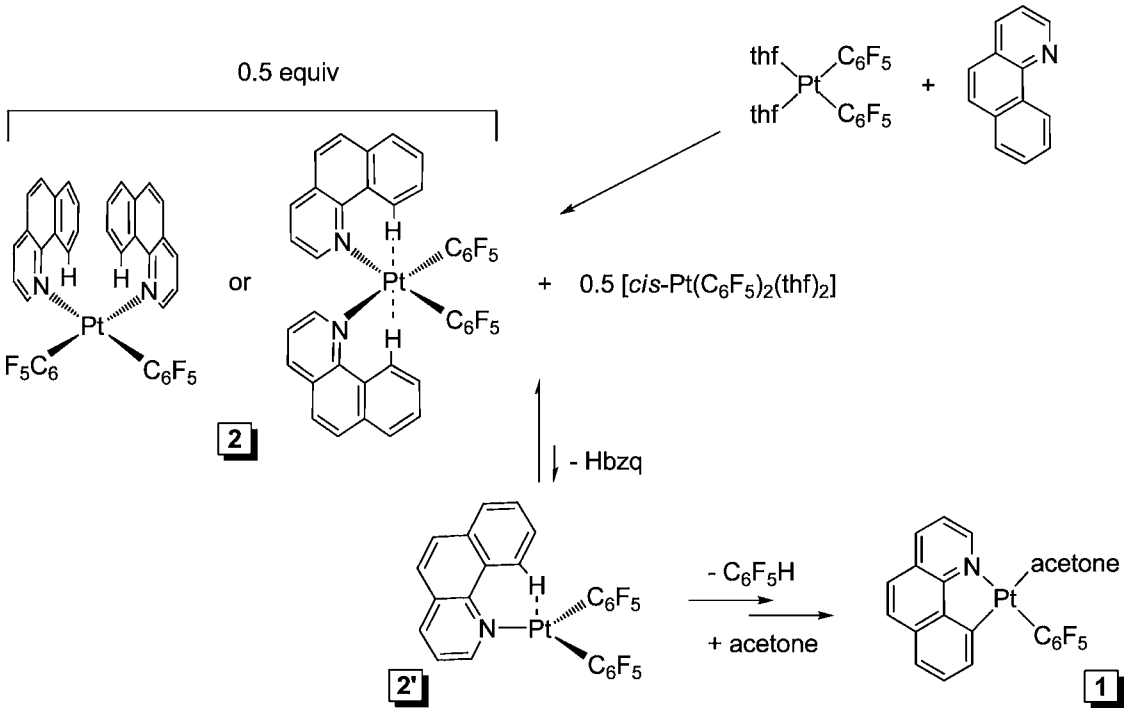

dx.doi.org/10.1021/ic301563u | *Inorg. Chem.* 2012, 51, 11665−11679

Scheme 3

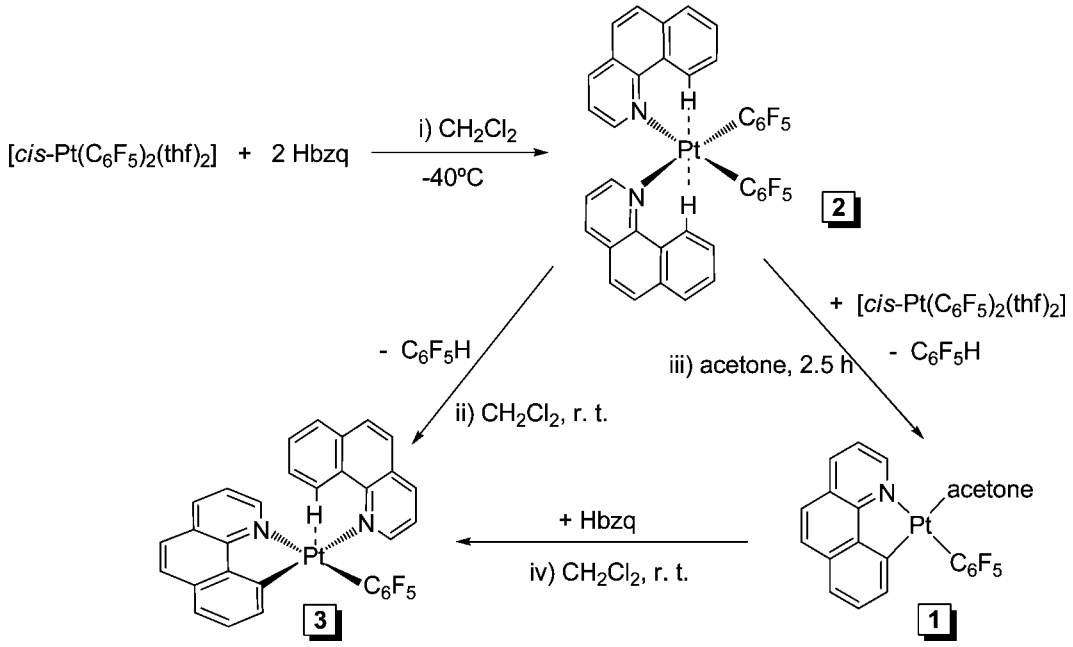

only were successful in obtaining suitable X-ray analysis crystals for $3{\cdot}0.25CH_2Cl_2$ (Figure 1).

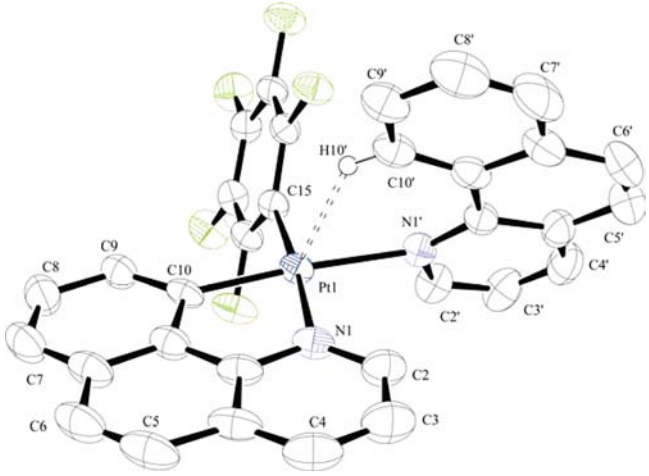

Figure 1. ORTEP view of the molecular structure of $[Pt(bzq)(C_6F_5)(Hbzq)]{\cdot}0.25CH_2Cl_2$ ($\mathbf{3}{\cdot}0.25CH_2Cl_2$). Ellipsoids are drawn at the 50% probability level. Hydrogen atoms are omitted for clarity. Selected bond distances and angles: Pt(1)–N(1′) 2.182(6), Pt(1)–N(1) 2.098(6), Pt(1)–C(10) 1.976(7), Pt(1)–C(15) 2.012(7), N(1)–Pt(1)–N(1′) 95.2(2), C(10)–Pt(1)–N(1) 81.7(3), C(15)–Pt(1)–N(1′) 89.3(2), C(15)–Pt(1)–C(10) 93.8(3).

The X-ray structure confirms the C–H activation of one of the 7,8-benzo[*h*]quinoline ligands and the N-coordination of the other one. In accordance with the spectroscopic data, the C_6F_5 group is coordinated in *cis* position to the metalated C(10) atom. The bond lengths and angles are in the range found for related complexes.[8a–e,11,12] The Pt–N(1′) bond length with the Hbzq ligand is relatively long [2.182(6) Å], reflecting the strong *trans* influence of the metalated C(10) atom of the bzq. This bond is longer than that found by Albinati and co-workers in $[trans\text{-}PtCl_2(Hbzq)(PEt_3)]$[22] [2.142(4) Å], the only crystal structure reported in platinum chemistry with a benzoquinoline acting as monodentate N-ligand. The roughly orthogonal coordination of the Hbzq ligand (dihedral angle 65.7°) places the H(10′) proton in a pseudoaxial position above the platinum coordination plane, being the Pt(1)–H(10′) vector which deviated only 23.4(1)° from the normal to this plane. The Pt(1)–C(10′) [3.241(9) Å] and Pt(1)–H(10′) [2.4508(3) Å] separations are comparable to those found in $[trans\text{-}PtCl_2(Hbzq)(PEt_3)]$ [Pt–C 3.189(7) Å; Pt–H ~2.53(8) Å], and fall in the range in which similar Pt···H bonding interactions have been reported in the literature.[19b,22,23] The Pt(1)···H(10′)–C(10′) is 142.9(6)°. Also interesting is the supramolecular packing of the platinum molecules, which stack in a head-to-head manner supported by $\pi\cdots\pi$(bzq) interactions [~ 3.5 Å; minimum C···C distance 3.46(1) Å] to give a columnar disposition through the *a*-axis (Figure 2), having influence on the luminescence properties of the complex (see Photophysical Studies section). Further inspection of the crystal structure reveals the presence of other types of noncovalent interactions [$\pi\cdots\pi(C_6F_5)$, C–H···F] generating a supramolecular 3-D network with vacant channels along the *a*-axis, in which the crystallization CH_2Cl_2 molecules accommodate (Figure S2 in Supporting Information).

Analytical and relevant spectroscopic data for **2** and **3** are collected in the Experimental Section and Supporting Information (^{1}H NMR spectra). For **2** two different conformers with the benzoquinoline ligand adopting a *syn* or an *anti* arrangement can be assumed (see Scheme 2), with the latter being more likely on the basis of steric (less $\pi\cdots\pi$ repulsion between the aromatic rings) and electronic (well directed Pt→H–C$^{10'}$ interactions) grounds. The ^{1}H and ^{19}F NMR spectra of **2** confirm the presence of only one set of signals for both ligands (Hbzq and C_6F_5), but only at low temperature (−40 °C) is the ^{19}F NMR spectrum consistent with a relatively rigid molecule in solution, exhibiting the expected set of five fluorine resonances (AFMRX system). By increasing the temperature, the two ortho and the two meta resonances broaden and coalesce (~293 K for the F_{ortho} and ~283 K for the F_{meta}, $\Delta G^{\ddagger}$ ~ 56.8 kJmol^{-1}), giving rise at room temperature to just three

dx.doi.org/10.1021/ic301563u | *Inorg. Chem.* 2012, 51, 11665–11679

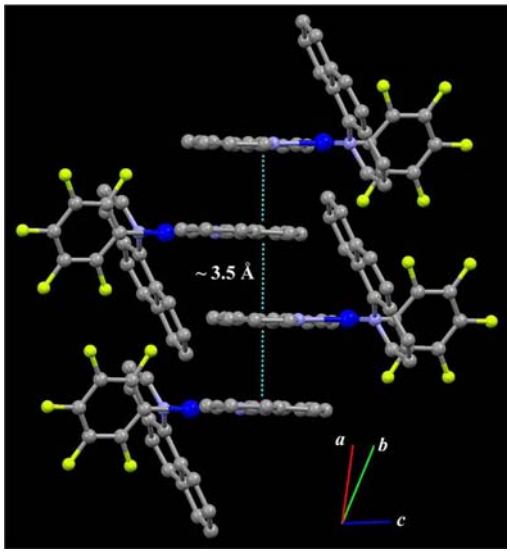

Figure 2. Detail of the intermolecular $\pi\cdots\pi$ stacking observed along the *a* axis for **3**·0.25CH_2Cl_2.

signals (AA′MXX′ system). The observed pattern at room temperature suggests that C_6F_5 rings behave as free rotating, a process which could take place directly in **2** or via a tricoordinated transient species **2′** in fast equilibrium with **2**. No detectable change was observed in the coalescence peak by diluting the sample by a factor of 2, thus excluding the occurrence of a dissociative process, at least to a significant extent. We note that the cyclometalation reaction, which transforms **2** into **3**, occurs very easily when the temperature is close to room temperature. In fact, signals due to **3** were also visible at the end of the temperature-dependent ^{19}F NMR studies. Not unexpectedly, the resonance due to the $H^{10'}$ proton appears (see Figure S3a) notably downfield shifted (δ 12.16) in relation to the free ligand (δ 9.30). In accordance to previous observations in related complexes, this fact indicates that the proton $H^{10'}$ is located in close proximity to the Pt center in a pseudoaxial position, experiencing the anisotropic deshielding associated to the Pt d_{z^2} electron density.[22−24] This arrangement could favor the proton transfer to the Pt center, lowering the energetic barrier for cyclometalation, in accordance with the ease cyclometalation observed for complex **2** (**2**→**3**). However, despite the remarkable deshielding observed for $H^{10'}$, no coupling to ^{195}Pt is observed. As a consequence, we cannot conclude that a Pt→H interaction exists in solution.[23b,c] In the case of **3**, the presence of both the deprotonated bzq^- and Hbzq is clearly observed in its proton NMR spectrum (see Figure S3b for details). As can be seen, some broadening due to platinum coupling is apparent at the base of the $H^{10'}$ signal (δ 12.44), but the expected coupling cannot be accurately calculated. The presence of five distinct signals in the ^{19}F NMR spectrum of **3** is a clear indication of the absence of free rotation of the C_6F_5 ring around the Pt−C_{ipso} bond, probably due to steric hindrance of the Hbzq.

Preparation and Characterization of Alkyne Platinum Complexes 4−7. The synthesis of platinum alkynyl based complexes has been extensively researched because of their rich structural diversity and chemical reactivity, and more recently because of the potential of these systems in the design of new molecular site electronic devices.[2e,h−m,14,25] Extensive work in this topic made by our group and others has shown the ability of metalla-alkynyl (M—C≡CR) and phosphino-alkynes (M—PR_2—C≡CR′) to coordinate to Pt(II), leading to a variety of polynuclear systems, some of which have intriguing photophysical properties.[2e,k,14a,c,25a,c] However, in spite of the similarity of these units and simple alkynes, the number of η^2-alkyne-Pt(II) complexes remains relatively scarce, and most of them have been confined to internal alkynes.[13,14,24] Experimental evidence supported by theoretical calculations indicates that the Pt(II)-η^2(alkyne) bonding interaction is weak, probably due to the low d_π back-donation from Pt(II) to the $\pi^*_{\parallel}$ and the presence of a four-electron destabilization interaction between the occupied $\pi_\perp$ of the alkyne and the other symmetry adopted filled metal dπ orbital.[26] In fact, the coordinated terminal alkyne has been found to be reasonably stabilized only in electron-rich anionic[13a,b] or five-coordinated[13c−e] fragments. With cationic and even neutral fragments the electrophilicity of the alkyne is notably enhanced upon coordination to Pt(II), providing the access to di-, oligo-, or polymerization of alkynes or the entry to interesting complexes, which are usually initiated by nucleophilic attacks or insertion reactions.[14,27] Due to the electronic characteristic of the C_6F_5 groups and strength of the Pt−C_6F_5 bond, Forniés et al. have demonstrated that the neutral "*cis*-Pt$(C_6F_5)_2$" and the anionic $[Pt(C_6F_5)_3]^-$ fragments are adequate synthons for the isolation of complexes containing two or one η^2-coordinated internal alkynes.[24b,c] In this context, we considered of interest (i) the use of the solvate complex **1**, having a C_6F_5 group, as a precursor for η^2-alkyne complexes, and (ii) the study of the photophysical properties of the final alkyne−benzoquinolate species. As possible alkynes we have chosen internal (PhC≡CPh) and terminal (HC≡CPh, HC≡C^{t}Bu, HC≡CFc) ones.

Complex **1** reacts with equimolar amounts of terminal alkynes HC≡CR (R = Ph, ^{t}Bu, Fc) and with diphenylacetylene (PhC≡CPh) in CH_2Cl_2 to produce the corresponding η^2-alkyne complexes [Pt(bzq)$(C_6F_5)(\eta^2$-HC≡CR)] (R = Ph **4**, ^{t}Bu **5**, Fc **6**) and [Pt(bzq)$(C_6F_5)(\eta^2$-PhC≡CPh)] **7**, respectively (Scheme 4 and Experimental Section). Although all attempts to obtain crystals of complexes **4**−**7** were unsuccessful, their formulation as η^2-alkyne derivatives shown in Scheme 4 was clearly confirmed by analytical and spectroscopic means. The IR spectra show a characteristic ν(C≡C) stretching band (1974−2017 cm^{-1}), which is shifted to lower frequencies in relation to free alkynes ($\Delta\nu$ 104−193 cm^{-1}), confirming the η^2-coordination of the ligands. Similar

Scheme 4

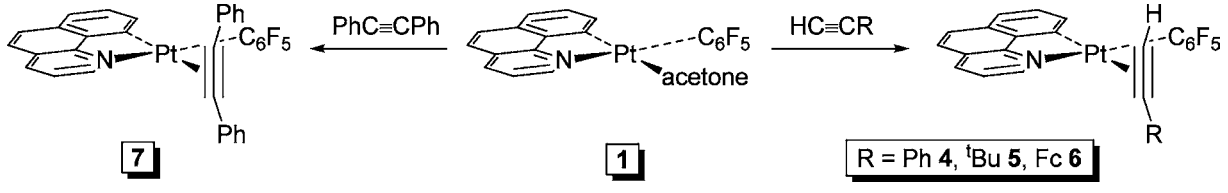

dx.doi.org/10.1021/ic301563u | *Inorg. Chem.* 2012, 51, 11665−11679

wavenumbers were reported for other platinum(II) alkyne complexes.[13b] In the case of **4**–**6**, containing terminal alkyne ligands, one (3233 **4**, 3215 cm^{-1} **6**) or two (3253, 3245 cm^{-1} **5**) ν(≡C—H) stretching bands were also observed, which are also lowered (Δ 56–68 cm^{-1}) with respect to the free ligands. Coordination of the terminal alkyne ligands is clearly inferred from proton NMR spectroscopy. Thus, the terminal acetylenic protons appear as a singlet in the range δ 4.15–4.91 with characteristic platinum satellites [$^2J_{Pt-H}$ = 46–50 Hz] (see Figure S4 for **4**). Interestingly, the observed coordination induced downfield shift ($\Delta\delta$ 1.83 **4**, 2.07 **5**, 1.7 **6**) is clearly larger than those reported for anionic complexes [K(18-cr-6)][$PtCl_3$(HC≡CR)][13b] ($\Delta\delta$ 0.8–1.0 ppm) and some five-coordinate derivatives such as [PtX_2(Me_2phen)(η^2-HC≡CPh)] ($\Delta\delta$ 0.64 ppm).[13c] However, the values of the platinum coupling constant are slightly smaller (46–50 Hz in **4**–**6** vs 66–70 Hz in [K(18-cr-6)][$PtCl_3$(HC≡CR)] or 54 Hz in [PtX_2(Me_2phen)(η^2-HC≡CPh)]), a fact likely due to the relatively high *trans* influence of the metalated carbon atom. Due to solubility reasons, only the $^{13}C\{^1H\}$ NMR spectrum of **5** was recorded. This complex showed the signals of the two acetylenic carbons at 65.7 (≡CH) and 95.1 (^{t}BuC≡), respectively, but despite prolonged accumulation no satellites were observed. The presence of five distinct signals in the ^{19}F NMR spectrum of **5** (R = ^{t}Bu) is a clear indication of the absence of free rotation about both the Pt(II) alkyne and the Pt–C_{ipso}(C_6F_5) bonds. However, in the case of complexes **4** and **6** with lesser bulky substituents, the environments of the two F_{ortho} (and the two F_{meta}) atoms are averaged. Although the observed pattern could be attributed to a lower energetic barrier to the rotation of the C_6F_5 ring in these complexes, the occurrence of free alkyne rotation cannot be excluded.

As has been noted before, terminal alkyne Pt(II) complexes are very rare, though they have been suggested in many stoichiometric and catalyst systems as initial transient species formed by displacement of labile molecules (solvent, olefin) in the precursors.[13b–d,27a,c] An easy isomerization of the initial η^2-alkyne to an α-carbocationic or η^1-vinylidene species as key reactive intermediate complex has been proposed to rationalize the observed nucleophilic addition to the C^α carbon atom.[14c,27c,28] Although some recent theoretical calculations have been shown that this η^2-alkyne to η^1-vinylidene equilibration on the Pt(II) sphere is crucial in some catalytic processes,[29] the experimental evidence is limited to complex [$Pt(CH_3)(PPh_3)_2$(C=CHPh)]$^+$, which has been detected by NMR spectroscopy at low temperature.[30] In order to rationalize the formation of the η^2-alkyne complexes **4**–**6**, we decided to examine the relative stability of the [Pt(bzq)(C_6F_5)(η^2-HC≡CPh)], **4**, and [Pt(bzq)(C_6F_5)(=C=CHPh)], **4′**, isomers using density functional theory calculations (DFT). Calculations were performed (Gaussian03/B3LYP/LanL2DZ) in the gas phase, and the results are collected in the Supporting Information (Figure S5, Tables S1–S3). The minimum-energy structure for both isomers (Figure S5) exhibits the expected features. For **4**, the alkyne is almost perpendicular to the complex plane (81.72°), with Pt–C (2.282, 2.408 Å) bond lengths similar to those found in [*cis*-$Pt(C_6F_5)_2$($PhC\equiv CPh)_2$] [2.311(5), 2.269(5) Å],[24c] but clearly longer to those reported for anionic alkyne derivatives [PtX_3(RC≡CR)]$^-$ (X = Cl,[24a] C_6F_5[24b]) (2.103–2.250 Å),[24a,b] thus reflecting the enhanced electrophilic character of the Pt in the neutral "Pt(bzq)(C_6F_5)" fragment. As expected, **4′** displays a nearly lineal geometry (Pt=C=C 176.04°) with the vinylidene plane approximately perpendicular to the platinum coordination plane (80.91°) and a Pt=C distance (1.911 Å), comparable to those reported, for instance, in platinum alkoxycarbene compounds.[31] The distinct electronic requirements of both ligands are reflected in the Pt–C(bzq) bond distances (2.023 Å **4** vs 2.069 Å **4′**), which are in agreement with the lower *trans* influence of the η^2-alkyne ligand. The comparison of the energies of both isomers indicates that the alkyne form **4** is ∼9.2 kcal/mol (9.6 kcal/mol after ZPVE corrections) more stable than the corresponding vinylidene isomer **4′**. This fact, which is a further support of the formulation of **4**–**6** as η^2-alkyne complexes, may be attributed to the strong electron-withdrawing properties of the bzq and C_6F_5 groups. The presence of these groups and the better π-acceptor properties of vinylidene ligands relative to alkynes would disfavor the typical tautomerization observed in other systems.

It is worth noting that complexes **4**–**7** are moderately stable in solid state, but not in solution. Thus, in tetrahydrofuran only the *tert*-butylalkyne complex **5** remains unaltered [δ ≡C–H 4.90, $^2J_{Pt-H}$ = 48 Hz]. In this solvent, the alkyne derivatives **4**, **6**, and **7** and the acetone solvate **1** display identical ^1H (bzq region) and ^{19}F NMR spectra, thus indicating that these complexes undergo ligand substitution, to yield the new solvate species [Pt(bzq)(C_6F_5)(thf)] in thf solution. In $CDCl_3$ solution, the stability of the terminal alkyne complexes decreases in the order **5** > **6** > **4**, giving rise to a complex mixture of products in which only complex [Pt(bzq)(C_6F_5)(Hbzq)] (**3**) and HC_6F_5 were detected by NMR spectroscopy. For comparison, after 2 h the most stable **5** remains unaltered, meanwhile **4** shows decomposition (∼ 10%). After 20 h only minor decomposition was observed for **5** (∼ 10%), while in the same time **4** had disappeared completely. The formation of **3** and HC_6F_5 in solution suggests the occurrence of alkyne (sp) C–H activation, likely via an oxidative addition, yielding a Pt(IV) hydride–acetylide pentacoordinate intermediate species, which could evolve through sp^2 C–H reductive coupling to form HC_6F_5 or Hbzq. Ease alkyne substitution by Hbzq in the precursor would explain the formation of **3**.

As was mentioned above, all attempts to obtain crystals suitable for X-ray diffraction studies of complexes **4**–**7** have been fruitless. Surprisingly, by slow diffusion (∼1 month) of *n*-hexane into a $CHCl_3$ solution of the ferrocenylalkynyl derivative **6** at low temperature (−30 °C), a small amount of orange crystals grew on the walls, which were identified by single-crystal X-ray diffraction methods as the unusual dinuclear product [Pt(κN:η^2-bzq-C≡CFc)(C_6F_5)(μ-κC^α:η^2-C≡CFc)Pt(bzq)(C_6F_5)], **8**. Unfortunately, we were not able to isolate enough of pure complex **8** for a complete spectroscopic characterization. The molecular structure of **8** is depicted in Figure 3, and selected structural parameters are given in Table 1. As is shown in Figure 3, in this evolution product **8**, the neutral "Pt(1)(bzq)(C_6F_5)" fragment is η^2 linked to the ferrocenyl alkynyl ligand of an unexpected ferrocenylacetylide Pt(2) unit [Pt(2)(bzq-C≡CFc)(C_6F_5)(C≡CFc)], which contains a rare functionalized 10-ferrocenylethynylbenzo[*h*]quinoline molecule bound in a chelating κN:η^2-(C≡C) fashion.

Carbon(sp^2)–carbon(sp) alkyne coupling is an important reaction to synthesize asymmetrical alkynes, which is usually catalyzed by copper salts and/or palladium complexes.[32] Nevertheless, though a wide variety of products have been found by reaction of transition metals with alkynes due to their very rich chemistry, we are not aware of the formation of a

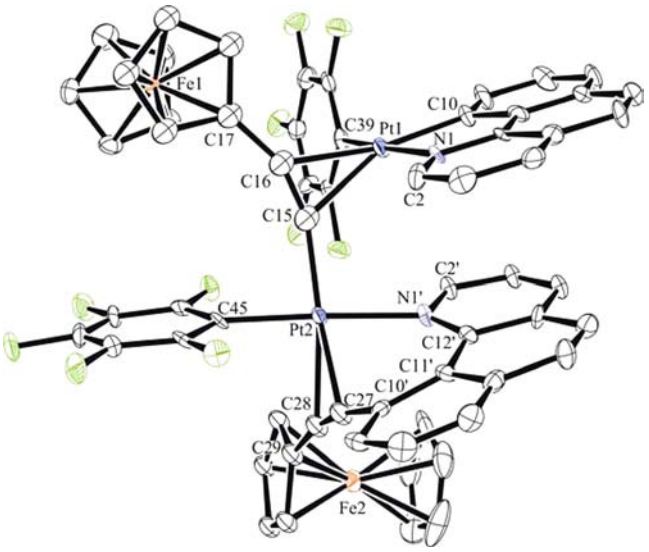

Figure 3. Molecular structure of $[Pt(\kappa N{:}\eta^2\text{-bzq-C}{\equiv}\text{CFc})(C_6F_5)(\mu\text{-}\kappa C^{\alpha}{:}\eta^2\text{-C}{\equiv}\text{CFc})Pt(bzq)(C_6F_5)]\cdot 2.5CH_2Cl_2\cdot H_2O$ (**8**·2.5CH_2Cl_2·H_2O). Ellipsoids are drawn at the 50% probability level. Hydrogen atoms are omitted for clarity.

Table 1. Selected Distances (Å) and Angles (deg) for Complex 8·2.5CH_2Cl_2·H_2O

Pt(1)−C(10)	2.030(8)	Pt(1)−N(1)	2.108(7)
Pt(1)−C(15)	2.247(10)	Pt(1)−C(16)	2.223(9)
Pt(1)−C(39)	1.995(8)	Pt(2)−C(15)	1.989(9)
Pt(2)−N(1′)	2.146(6)	Pt(2)−C(45)	2.014(8)
Pt(2)−C(27)	2.171(9)	Pt(2)−C(28)	2.228(9)
C(15)−C(16)	1.219(12)	C(16)−C(17)	1.441(12)
C(10′)−C(27)	1.438(11)	C(27)−C(28)	1.227(12)
C(28)−C(29)	1.425(12)		
N(1)−Pt(1)−C(10)	80.9(3)	C(39)−Pt(1)−C(10)	85.5(3)
N(1′)−Pt(2)−C(15)	96.9(3)	C(15)−Pt(2)−C(45)	92.7(3)
Pt(2)−C(15)−C(16)	160.4(9)	C(15)−C(16)−C(17)	155.4(10)
C(10′)−C(27)−C(28)	168.2(9)	C(27)−C(28)−C(29)	167.3(9)

coordinated functionalized alkynyl-benzoquinoline molecule such as bzq(C≡CFc)-10. The formation of the ferrocenyl ethynylbenzo[*h*]quinoline implies a formal C(sp^2)−C(sp) coupling, which is likely caused by an initial C−H alkyne activation via oxidative addition to the Pt(II)(2) center, which end up with C(bzq)−C(alkyne) reductive elimination. The presence of an additional C≡CFc group σ-bonded to Pt(2) indicates a formal hydrogen elimination process with a second alkyne molecule, which would take place in a mono- or bimetallic species. In this regard, it is worth mentioning that recently Ritter and co-workers have found that free 10-chlorobenzo[*h*]quinoline Clbzq is generated by oxidation of $[Pd(bzq)(OAc)]_2$ with $PhICl_2$, and they have shown that the reductive Cl−C bond elimination occurs via a dinuclear symmetrical intermediate $[Pd_2^{III}(bzq)_2Cl_2(OAc)_2]$ complex.[33]

The structural details of **8** are those expected. Thus, the Pt(1)−acetylide bond lengths [2.247(10), 2.223(9) Å] and the bent back angles at C^{α} [160.4(9)°] and C^{β} [155.4(10)°] are comparable to those observed in $[(OC)(C_6F_5)_2Pt(\mu\text{-C}{\equiv}\text{CPh})Pt(C{\equiv}\text{CPh})(PPh_3)_2]$[34] [2.268(1), 2.257(10) Å; 165.0(9)°, 157.9(10)°], and as expected, the alkynyl vector is essentially perpendicular to the Pt(1) coordination plane [75.1(6)°]. The chelate ($\kappa N{:}\eta^2$-C≡C) bzqC≡CFc ligand is notably twisted by coordination of the alkyne unit to Pt(2) [dihedral angle between the planes formed by the atoms C2′−N1′−C12′ and C10′−C27−C28 of 67.1(5)°]. The location of the alkyne unit is constrained by ring limitations, but is coordinated virtually orthogonal to the coordination plane [67.5(5)°]. The Pt(2)−alkyne bonds lengths [2.171(9) and 2.228(9) Å] and the back bending at the C(27) [168.2(9)°] and C(28) [167.3(9)°] alkyne carbons are similar to those found in other alkyne Pt(II) complexes.[24a] The Pt···Pt distance is very long [3.783(1) Å], but the bzq and bzqC≡CFc are stacked at relatively close distance [∼ 3.4 Å, minimum C···C distance 3.40(1) Å, N−N 3.32(1) Å], suggesting the occurrence of *intramolecular* $\pi\cdots\pi$ interactions. The analysis of the packing reveals also the presence of *intermolecular* $\pi\cdots\pi$ interactions (see Figure S6 in Supporting Information).

Photophysical Studies. *Absorption Spectra.* The data obtained for the electronic absorption spectra of all complexes (CH_2Cl_2 or (2-Me)thf solutions) are summarized in Table S4. The spectra of **1**−**3** in (2-Me)thf are shown in Figure 4,

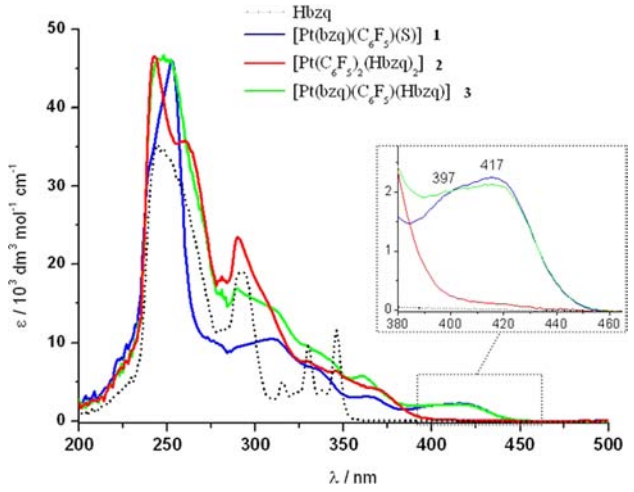

Figure 4. Normalized UV−vis absorption spectra of **1**−**3** in (2-Me)thf (5×10^{-5} M) at 298 K. In the inset: low-energy region.

whereas those of the η^2-alkyne complexes **4**−**7** in CH_2Cl_2 solution are collected in Figure S7. For comparison, the spectrum of Hbzq ligand is included in Figure 4. As is shown in this figure, complexes **1**−**3** give intense absorptions ($\varepsilon > 20\,000$ M^{-1} cm^{-1}) in the range 243−370 nm, attributable to metal perturbed $\pi-\pi^*$ intraligand (^{1}IL, Hbzq, bzq, C_6F_5) transitions. The cyclometalated complexes **1** and **3** exhibit two additional and less intense (ε = 1.9−2.3 × 10^3 M^{-1} cm^{-1}) low-energy absorptions located at similar energies (397, 417 nm), which, on the basis of theoretical calculations and previous assignments, are attributed to an admixture of ^{1}IL and metal-to-ligand charge transfer (^{1}MLCT).[8c,e,35]

As illustrated in Figure S7, coordination of the alkyne ligands HC≡CR (R = Ph **4**, ^{t}Bu **5**) and PhC≡CPh (**7**) causes only minor modifications on the low energy region in relation to the precursor **1**. However, this band appears slightly shifted in the *tert*-butyl alkyne derivative (406 nm) in relation to **4** and **7** (399 nm), containing the less donor phenyl and diphenylalkyne, suggesting some alkyne-to-bzq contribution. According with theoretical calculations (TD-DFT) for complex $[Pt(bzq)(C_6F_5)(\eta^2\text{-HC}{\equiv}\text{CPh})]$ **4**, this band has mainly intraligand character (^{1}IL, bzq), with some metal-to-ligand ^{1}MLCT and ligand'-to-ligand (C_6F_5/alkyne→bzq) contribution. For the

dx.doi.org/10.1021/ic301563u | *Inorg. Chem.* 2012, 51, 11665−11679

Table 2. Photophysical Data for Complexes 1−5 and 7[a]

compd	medium (T/K)	λ_{em}/nm (λ_{exc}/nm)	τ/μs
[Pt(bzq)(C_6F_5)(acetone)] **1**	solid (298)	480, 515, 585_{max} (400)	13.2 (480)
	solid (298)	∼595 (445−475)	16.5 (585)
	solid (77)	506_{max}, 540, 580sh (400)	157
	(2-Me)thf (298)	482_{max}, 507, 578sh (400)	8.4
	(2-Me)thf (77)	477_{max}, 514, 553, 598sh (490)	388
[Pt(C_6F_5)$_2$(Hbzq)$_2$] **2**	solid (298)	545 (400)	9.1
	solid (77)	508, 532_{max}, 572sh (400)	341 (52%), 51.8 (48%) (532)
	solid (77)	570 (470)	20.1
	(2-Me)thf (77)[b]	479_{max}, 517, 554, 600sh (400)	376
[Pt(bzq)(C_6F_5)(Hbzq)] **3**	solid (298)	496, 595_{max} (400)	9.0 (495)
	solid (298)	595 (450−480)	14.5
	solid (77)	507_{max}, 544, 586sh (400)	186
	(2-Me)thf (298)	485_{max}, 510 (400)	9.2
	(2-Me)thf (77)	480_{max}, 515, 555, 600sh (400)	428
[Pt(bzq)(C_6F_5)(η^2-HC≡CPh)] **4**	solid (298)[c]	609 (400−470)	12.8
	solid (77)	510, 575_{max}, 610 (380)	167 (510)
	solid (77)	555_{sh}, 575, 610 (440)	112 (575); 65.2 (610)
	CH_2Cl_2 (298)[d]	474 (370−440)	10.0
	CH_2Cl_2 (77)[d]	474_{max}, 510, 550, 600sh (370−440)	342
[Pt(bzq)(C_6F_5)(η^2-HC≡C^{t}Bu)] **5**	solid (298)[c]	600 (400−470)	13.9
	solid (77)	481, 500_{max}, 523, 538 (380)	76.9 (500)
	solid (77)	481, 500_{max}, 523, 538, 613_{max} (440)	42.8 (613)
	CH_2Cl_2 (298)[e]	482 (370−440)	11.3
	CH_2Cl_2 (77)[e]	479_{max}, 515, 554, 600	299
[Pt(bzq)(C_6F_5)(η^2-PhC≡CPh)] **7**	solid (298)[c]	565, 625_{max} (400−470)	11.1 (565); 29.5 (23%), 5.0 (77%) (625)
	solid (77)	520_{max}, 555 (400)	41.7 (520); 42.1 (555); 47.9 (605)
	solid (77)	555_{max}, 605 (440)	
	CH_2Cl_2 (298)[e]	482 (370−440)	10.8
	CH_2Cl_2 (77)[e]	478_{max}, 512, 551, 600_{sh} (370−440)	302

[a] **1−3**, 10^{-3} M; **4−7**, 10^{-4} M solutions. [b] Not emissive at 298 K. [c] Weak. [d] In 2-Me(thf) solutions (298 K): 484_{max}, 505 (370−440 nm); (77 K) 477_{max}, 512, 552, 600sh (370−440 nm). [e] Similar pattern in 10^{-4} M 2-Me(thf) solutions.

ferrocenyl alkyne complex **6**, a similar band is also found at *ca.* 394 nm. As is typical in Fc containing complexes, this derivative exhibits a lower and very weak energy band at 465 nm ($\varepsilon \sim 500$ $M^{-1}cm^{-1}$) attributed, according to previous assignments,[36] to a ^{1}MLCT transition with some d−d character on the C≡CFc group.

Emission Spectra. Complexes **1−3** exhibit luminescence in the solid state and in solution at room temperature and at low temperature (77 K) (Table 2). The cyclometalated complexes **1** and **3** show in solid state at 298 K an emission profile with two different bands, related to different excitation profiles. Upon excitation at 400 nm, they exhibit a long-lived high-energy emission band (480, 515 nm **1**, 496 nm **3**), ascribed to a typical mixed ^{3}IL/^{3}MLCT excited state, and a prominent low-energy unstructured band centered at ∼595 nm, which can be selectively obtained by increasing the wavelength of excitation (Figure 5 for **3** and Figure S8 for **1**). The shape and energy of this low energy band, together with the presence of extended close $\pi\cdots\pi$ (bzq) interactions observed in **3**, are suggestive of the occurrence of aggregation-induced $\pi\cdots\pi$ emission in solid state, as has been supported by DFT calculations. Upon cooling at 77 K, the emissions are more intense and turn visually into green. The low-energy band disappears, showing only the structured high emission band slightly red-shifted (506, 540, 580sh **1**; 507, 544, 586sh nm **3**), with long lifetimes (157 μs **1**, 186 μs **3**) indicative of emission having predominant ^{3}IL parentage. Probably, the access to the low energy aggregation-induced $\pi\pi$ emission is less effective at 77 K than at 298 K,

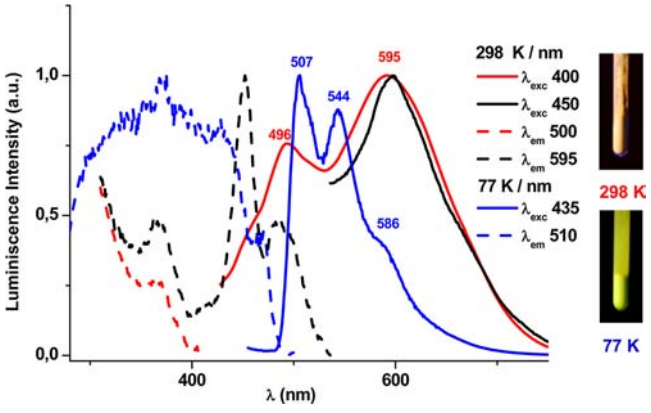

Figure 5. Normalized excitation and emission spectra of [Pt(bzq)-(C_6F_5)(acetone)] **3** in solid state at 298 and 77 K.

being responsible of the observed thermochromic behavior. Both complexes (**1** and **3**) exhibit similar profiles in diluted (5×10^{-5} M) or concentrated (10^{-3} M) (2-Me)thf solutions (see Table 2). They show at 298 K a slightly structured band in the green region (∼500 nm) with lifetime measurements in the microsecond range (8−9 μs), which becomes better structured Figure S9) in glass state (77 K). The absence of rigid-ochromism, together with the extremely long lifetimes (388 μs **1**, 428 μs **3**), which fit well to monoexponential decays (Figure S10), are indicative of emission with primarily ^{3}IL parentage.

dx.doi.org/10.1021/ic301563u | *Inorg. Chem.* 2012, 51, 11665−11679

Complex [*cis*-Pt(C_6F_5)$_2$(Hbzq)$_2$] (**2**) exhibits in solid state at 298 K only a very weak emission (~545 nm) of difficult assignment, probably due to the lack of the cyclometalate group. At 77 K (Figure S11), the intensity of the emission increases, and two different bands, depending on the λ_{exc} used, are observed. By excitation at λ_{exc} 400 nm, it shows a structured emission band (508, 532 nm) with a long lifetime [341 (52%), 51.8 (48%) μs] being attributed to a ^{3}IL (Hbzq) excited state. However, excitation at lower energies (λ_{exc} 470 nm) results in an unstructured emission band centered at 570 nm, with a shorter lifetime (20 μs). The excitation spectrum corresponding to this 570 nm band (Figure S11) extends to ~500 nm, suggesting that this low energy emission could be likely associated to the occurrence of close $\pi\cdots\pi$ interactions between aromatic Hbzq ligands in solid state. In solution, complex **2** is only emissive in glass state exhibiting a similar long-lived (376 μs) structured ^{3}IL emission to that observed for **1** and **3**.

With the exception of the ferrocenyl complex **6**, the η^2-alkyne derivatives (**4**, **5**, and **7**) are also photoluminescent in solid state and in solution at 298 and 77 K. The lack of luminescence in **6** is not unexpected and could be attributed to the presence of Fc group, which deactivates the excited state through nonradiative routes.[37] Complexes **4** and **5** show in solid state at room temperature a weak long-lived (12.8 μs **4**, 13.9 μs **5**) low-energy emission (609 nm **4**, 600 nm **5**), likely dominated by an excited state associated with the presence of a certain degree of $\pi\cdots\pi$ intermolecular contacts, which usually shift to the red the typical ^{3}MLCT and/or ^{3}LL′CT excited states (Figure S12). Upon cooling to 77 K, this emission changes to a more intense typical structured ^{3}IL/^{3}MLCT in **5** (500 nm, τ 76.9 μs), whereas in **4** both emissions due to the monomer (minority, 510 nm, τ 167 μs) and $\pi\cdots\pi$ aggregation (majority, 575–605 nm, τ 65.2 μs) are still observed (see Figure S12). The solid diphenylalkyne complex **7** exhibits at room temperature a broad asymmetric emission, with two maxima at 565 nm (τ 11.1 μs) and 625 nm [29.5 (33%), 5 (77%) μs], which clearly resolves into two different structured emissions at 77 K. As can be seen in Figure 6, these emissions are related with different excitation profiles, suggesting the presence of two close nonequilibrated excited states, tentatively attributed to mixed ^{3}IL/^{3}MLCT and ligand′-to-ligand ^{3}L′LCT (L′ = C≡C) excited states, respectively.

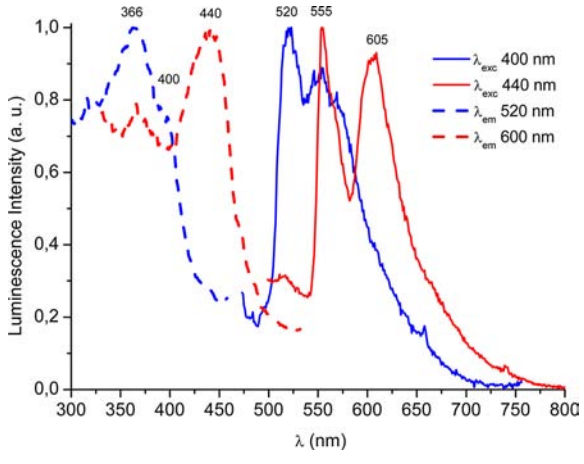

Figure 6. Normalized excitation and emission spectra of [Pt(bzq)-(C_6F_5)(η^2-PhC≡CPh)] (**7**) in solid state at 77 K.

As was expected, in fluid CH_2Cl_2 at 298 K, all alkyne complexes (**4**, **5**, and **7**) show an unstructured band (474 nm **4**, 482 nm **5**, 482 nm **7**) with an emission lifetime in the microsecond regime, which with reference to previous work in benzoquinolate Pt(II) complexes,[8a−e,h,11,12] is assigned to a mixed ^{3}IL/^{3}MLCT excited state (Figure 7). At 77 K, the

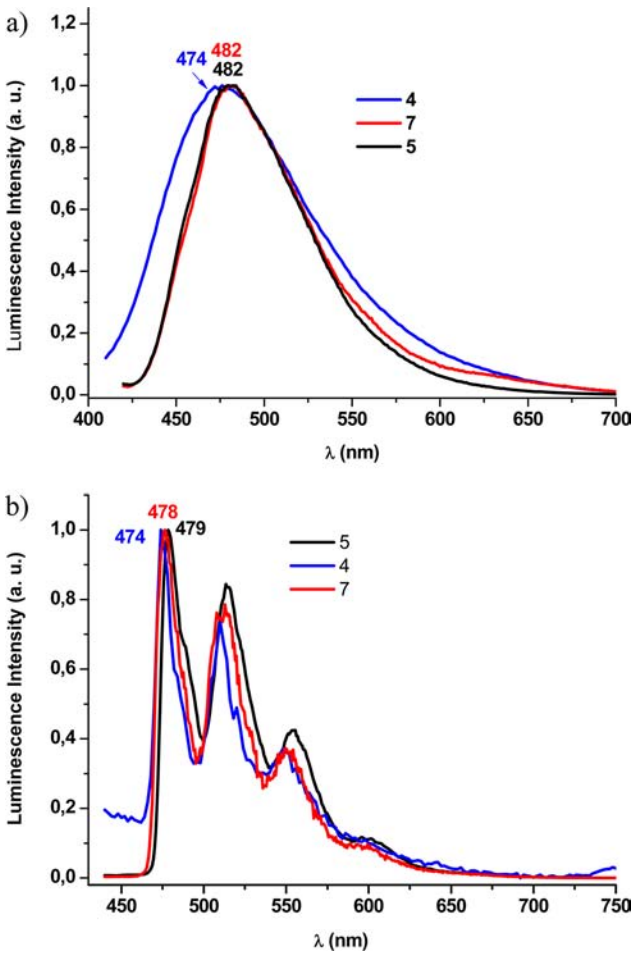

Figure 7. Normalized emission spectra of (a) **4** and (b) **5** in CH_2Cl_2 5 × 10^{-4} M at 298 K and at 77 K.

emission band becomes vibronically resolved (λ_{max} 474 **4**, 479 **5**, 478 nm 7). The very long lifetimes (~300 μs) and the negligible influence of the alkyne are indicative of a predominant ^{3}IL character (Figure 7). In (2-Me)thf fluid solution, **4** reproduces exactly the spectrum observed for **1** thus indicating, according also to the NMR data in d_6-thf, that the alkyne is substituted in solution by a solvent thf molecule, whereas **5** and **7** are stable in thf solution, displaying a similar profile to that described in CH_2Cl_2.

Theoretical Calculations. To gain further insight into the nature of the absorption and emission characters of these complexes in CH_2Cl_2 or (2-Me)thf a theoretical analysis based on a DFT (TD-DFT) approach was performed on selected complexes (**3**, **4**, and **6**). Structures (S^0 and T^1, Figures S13–S15), geometrical details (Table S5), and optimized coordinates (Table S6) are collected in the Supporting Information. The optimized geometry of **3** reproduces the one obtained by X-ray, including the dihedral angle between the Hbzq ligand and the bzq plane and the short Pt···H(bzq) contact [2.39931 Å in S^0, 2.39163 in T^1 vs 2.4508(3) Å in X-ray]. For the alkyne

dx.doi.org/10.1021/ic301563u | *Inorg. Chem.* 2012, 51, 11665–11679

Table 3. Composition (%) of Frontier MOs in the Ground State for Complexes 3, 3_2, 4, and 6 in Gas Phase

	3					3_2				
MO	eV	C_6F_5	Hbzq	Pt	bzq	eV	C_6F_5	Hbzq	Pt	bzq
LUMO + 3	−1.13	0	1	3	96	−1.55	0	42	2	56
LUMO + 2	−1.54	0	98	1	1	−1.56	0	2	2	96
LUMO + 1	−1.78	0	0	3	97	−1.99	0	100	0	0
LUMO	−1.99	0	99	1	0	−2.00	0	100	0	0
HOMO	−5.47	0	1	30	69	−5.41	0	2	26	72
HOMO − 1	−5.78	11	7	78	4	−5.42	0	2	28	70
HOMO − 2	−5.82	66	2	30	2	−5.76	4	6	84	6
HOMO − 3	−6.04	97	1	1	1	−5.77	4	8	82	6
	4					6				
	eV	C_6F_5	Pt	bzq	H—C≡CPh	eV	C_6F_5	Pt	bzq	H—C≡CFc
LUMO + 3	−0.54	2	9	56	34	−0.53	2	8	59	30
LUMO + 2	−1.17	0	3	48	49	−0.65	0	4	13	83
LUMO + 1	−1.58	0	5	49	45	−1.42	0	5	85	10
LUMO	−1.98	1	4	92	3	−1.95	0	4	94	2
HOMO	−5.82	13	18	60	10	−5.49	1	2	2	95
HOMO − 1	−6.0	54	21	23	2	−5.54	0	1	1	98
HOMO − 2	−6.17	96	3	1	0	−5.85	6	14	67	12
HOMO − 3	−6.29	10	78	9	2	−6.00	56	24	15	5

complexes **4** and **6**, the expected perpendicular coordination of the alkyne to the platinum coordination was obtained. In the corresponding optimized T^1 state of **4** the most remarkable feature is the significant withdrawal of the C_β carbon atom (2.40791 in S^0 to 3.21623 Å in T^1).

The distribution of important frontier orbitals in the ground state and the corresponding partial molecular orbital composition (percentages), together with selected low-lying transitions for **3**, **4**, and **6**, are provided in Table 3 and in the Supporting Information (Tables S7−S8). For complex **3**, the HOMO has mixed Pt and bzq character whereas the LUMO and LUMO + 1, which are close in energy, are primarily located in the Hbzq and bzq ligands, respectively. The lowest energy singlet transition calculated in thf (390 nm) arises primarily from HOMO to LUMO + 1, therefore, supporting a mixed ^{1}MLCT (Pt→bzq)/^{1}IL(bzq) character for the experimental band located at 417 nm. Substitution of the Hbzq for the η^2-alkyne in **4** changes the nature of the LUMO (now located in the bzq anion) and of the HOMO, which contains significant contribution of the coligands (C_6F_5 13% and HC≡CPh 10%). The lowest-energy band, experimentally observed in CH_2Cl_2 at 399 nm, is consistent with the simulated at 374 nm. This band, which is blue-shifted in relation to **3** and primarily due to a HOMO→LUMO transition, can be characterized as a mixed ^{1}IL/^{1}MLCT with some ligand(C_6F_5, alkyne)-to-ligand(bzq) (^{1}L′LCT) character.

In complex **6**, with the η^2-HC≡CFc ligand, the first calculated allowed transition with strong oscillator strength is blue-shifted (366 nm) in relation to **4**, in agreement with that observed experimentally (394 nm). This band mainly originates from the HOMO − 2 to LUMO and can be also assigned as mixture ^{1}IL/^{1}MLCT with ^{1}L′LCT contribution.

We also investigated the emission properties by optimization of the lowest-energy triplet state (T^1) for complexes **3** and **4** using the unrestricted U-B3LYP method (Table S5, Figures S13, S14). The calculated emission energies, as the difference between the energy of the T^1 and the energy of the singlet state with the triplet state optimized geometry (544 nm thf **3**, 504 nm CH_2Cl_2 **4**), are qualitatively close to the experimental values (485 nm (2Me)-thf **3**, 482 nm CH_2Cl_2 **4**). As can be seen in Figure 8 for complex **3**, the LSOMO (HOMO in S^0 notation) is essentially analogous to the HOMO in the ground state, being located on the bzq and the Pt. However, the HSOMO (LUMO in S^0 notation) has a different contribution to the LUMO in the ground state, since after the triplet optimization the unoccupied orbital centered on the bzq ligand (LUMO + 1 in S^0) is stabilized, becoming the HSOMO in T^1. Therefore, we conclude that the emission in complex **3** is due to a ^{3}IL excited state (L = bzq) with some mixing ^{3}MLCT. For **4**, the HSOMO and LSOMO orbitals in the optimized T^1 state are mainly centered on the bzq ligand (Figure S16, HSOMO = bzq 83%, HC≡CPh 10%, Pt 7%; LSOMO = bzq 83%, HC≡CPh 5%, Pt 12%) supporting an ^{3}IL origin for its emission with a negligible contribution of the alkyne unit.

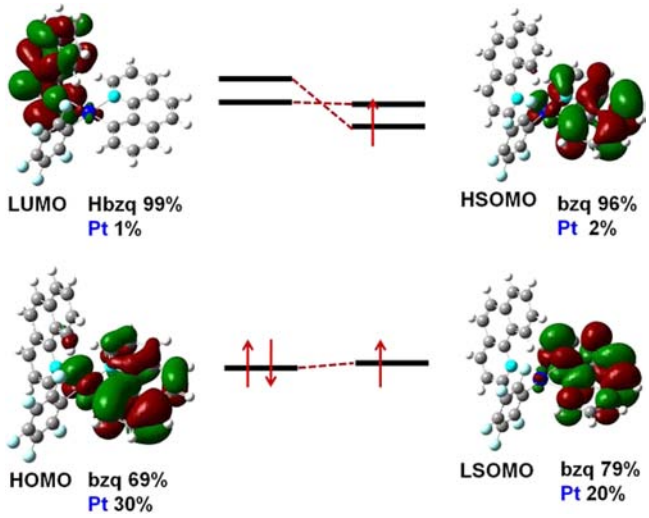

Figure 8. Molecular orbital plots for the computed S^0 and T^1 states of complex **3**.

To interpret the low energy emissions observed in solid state at room temperature not only for **3**, but also for **1** and the

dx.doi.org/10.1021/ic301563u | Inorg. Chem. 2012, 51, 11665−11679

alkyne derivatives, a DFT study was performed on a dimer $\mathbf{3}_2$ formed by two molecules of **3** stacked through the bzq ligands as a model of the extended chain observed in the crystal structure. On the basis of calculations (Table S6, Figure S17), we found that the frontier molecular orbitals (HSOMO and LSOMO) in the optimized T^1 state are delocalized over the two bzq ligands and the metal centers, having some degree of $\pi\cdots\pi$ bonding interaction (Figure S18). This fact is suggestive of stronger $\pi\cdots\pi$ interaction in the excited state, which is reflected in the shorter bzq···bzq separation in T^1 in relation to the ground state (see Table S9) and may be considered as the major cause for the substantial stabilization of the emitting state. This phenomenon has many precedents in square-planar Pt(II) complexes and recently has been also observed in phosphorescent Ir(III) complexes.[38] The room temperature solid-state emission can be ascribed to aggregation induced emission having strong platinum-to-ligand-ligand charge transfer (^{3}MLLCT).

CONCLUSIONS

In summary, an interesting platinum solvate complex [Pt(bzq)-(C_6F_5)(acetone)] **1** has been prepared by easy C−H activation of Hbzq using [*cis*-Pt(C_6F_5)$_2$(thf)$_2$] as precursor. We have found that the metalation involves the initial formation of the saturated complex [*cis*-Pt(C_6F_5)$_2$(Hbzq)$_2$] **2**, which subsequently reacts with additional [*cis*-Pt(C_6F_5)$_2$(thf)$_2$] to give **1** and C_6F_5H. Moreover, the isolation of **2** allows us to illustrate that the metalation on the electrophilic "*cis*-Pt(C_6F_5)$_2$" fragment is very effective as this complex evolves easily to the new derivative [Pt(bzq)(C_6F_5)(Hbzq)], **3**.

On the other hand, we have shown that the acetone molecule in **1** can be easily displaced by alkynes allowing the synthesis of [Pt(bzq)(C_6F_5)(η^2-RC≡CR′)] (**4**−**7**), which are the first reported η^2-alkyne-cycloplatinate complexes. The isolation of the terminal η^2-alkyne derivatives **4**−**6** is particularly rare, and their stability in relation to typical vinylidene isomers was addressed by DFT calculations in **4** and [Pt(bzq)(C_6F_5)(=C=CHPh)] **4**′. These η^2-alkyne complexes are only moderately stable in nondonor solvents, and in the case of **6**, it was found to evolve to the diplatinum complex [Pt(κN:η^2-bzq-C≡CFc)(C_6F_5)(μ-κC^{α}:η^2-C≡CFc)Pt(bzq)(C_6F_5)] (**8**) containing the unusual κN-η^2-bzqC≡CFc ligand. Further, studies aimed at generating functionalized benzoquinoline derivatives starting from **6** are in progress.

All complexes (except **6**) showed emissive properties in solution and glasses that originated mainly from intraligand (bzq) excited states with some mixing ^{3}MLCT, as supported by TD-DFT on selected complexes. Complexes **1** and **3** exhibit an interesting luminescent thermochromism in the solid state. This behavior has been rationalized (DFT calculations) in terms of the occurrence of aggregation induced emission, favored by intermolecular $\pi\cdots\pi$ stacking of adjacent bzq ligands, as supported by the crystal structure of **3**. At low temperature, both complexes (**1**, **3**) display the typical structured *green* emission due to admixture ^{3}IL/^{3}MLCT excited states, associated with essentially undisturbed monomer species. The *orange* emission observed at room temperature is associated with the participation of a low-lying emissive state, which delocalizes the electron density onto both adjacent bzq ligands [platinum ligand-to-ligand charge transfer (^{3}MLLCT) in nature].

EXPERIMENTAL SECTION

General Comments. All reactions were carried out under an atmosphere of dry argon, using standard Schlenk techniques. Solvents were obtained from a solvent purification system (M-BRAUN MB SPS-800). NMR spectra were recorded at 293 K on Bruker ARX 300 or ARX 400 spectrometers. Chemical shifts are reported in ppm relative to external standards ($SiMe_4$, $CFCl_3$), and all coupling constants are given in Hz. The NMR spectral assignments of the benzoquinolate ligand (bzq) follow the numbering scheme shown in Figures S1 and S3. IR spectra were obtained on a Nicolet Nexus FT-IR spectrometer, using nujol mulls between polyethylene sheets. Elemental analyses were carried out with Perkin-Elmer 2400 CHNS/O or Carlo Erba EA1110 CHNS-O microanalyzers. Mass spectra were recorded on a HP-5989B (ES) or a Microflex MALDI-TOF Bruker (MALDI) spectrometer operating in the linear and reflector modes using dithranol as matrix. The optical absorption spectra were recorded using a Hewlett-Packard 8453 (solution) spectrophotometer in the visible and near-UV ranges. Emission and excitation spectra were obtained on a Jobin-Yvon Horiba Fluorolog 3-11 Tau-3 spectrofluorimeter, with the lifetimes measured in phosphorimeter mode. 7,8-Benzoquinolate (Hbzq) was purchased from Sigma-Aldrich, and [*cis*-Pt(C_6F_5)$_2$(thf)$_2$] was prepared as reported previously.[39]

*Preparation of [Pt(bzq)(C_6F_5)(CH_3COCH_3)] (**1**).* 7,8-Benzoquinoline 0.16 g (0.89 mmol) was added to an acetone solution (20 mL) of [*cis*-Pt(C_6F_5)$_2$(thf)$_2$] (0.60 g, 0.89 mmol) and the mixture refluxed for 2.5 h. Then, the resulting yellow solution was evaporated to small volume (∼2 mL) and treated with 15 mL of *n*-hexane, to yield complex **1** as a microcrystalline yellow product (0.52 g, 97%). ^{1}H NMR (400 MHz, CD_3COCD_3, 20 °C, δ): 8.67 (d, $J \approx 8$, H^2, bzq), 8.66 (d, $J \approx 8$, H^4, bzq) (two overlapped signals), 7.87 (d), 7.79 (d) (J = 8.6, H^5/H^6, bzq), 7.75 (t, $J \approx 7$, H^3, bzq), 7.58 (d, J = 7.5, H^7, bzq), 7.26 (t, J = 7.4, H^8, bzq), 6.90 (d, J = 6.9, $^3J_{Pt-H}$ = 70, H^9, bzq), 2.06 (s, 6H, CH_3COCH_3). ^{19}F NMR (282.5 MHz, $CDCl_3$, δ): −40 °C, −118.4 (dd, $^3J_{Pt-F}$ = 513, 2*o*-F), −161.6 (t, *p*-F), −163.3 (m, 2*m*-F); 20 °C, −118.1 (d, $^3J_{Pt-F}$ = 501, 2*o*-F), −162.2 (t, *p*-F), −164.0 (m, 2*m*-F). ^{13}C{^{1}H} NMR (100.6 MHz, CD_3COCD_3, 20 °C, δ): 206.8 (s, CO, CH_3COCH_3), 155.3 (s, J_{Pt-C} = 108, C^{12}), 151.7 (dm, J = 228, C_6F_5), 148.3 (s, C^2), 142.8 (s, C^{10}), 139.9 (s, C^4), 138.5 (dm, C_6F_5), 135.4 (s, $^3J_{Pt-C}$ = 42, C^{14}), 135.3 (s, $^2J_{Pt-C}$ = 126, C^9), 131.0 (s, C^5 or C^6), 130.9 (s, $^3J_{Pt-C}$ = 89, C^8); 129.2 (s, C^{11}), 128.5 (s, $^3J_{Pt-C}$ = 25, C^{13}), 125.1 (s, C^5 or C^6), 123.8 (s, C^3), 123.2 (s, C^7), 31.6 (s, CH_3, CH_3COCH_3). IR (cm^{-1}): ν(CO) 1661(s), $\nu_{x\text{-sens}}$(C_6F_5) 802 (s). MS ES(−): *m*/*z* (%) 599 [M]$^-$, (17); 540 [M − (CH_3COCH_3)]$^-$ (5). Anal. Calcd (%) for $C_{22}F_5H_{14}NOPt$: C, 44.16; H, 2.36; N, 2.34. Found: C, 43.91; H, 2.29; N, 2.01%.

*Preparation of [cis-Pt(C_6F_5)$_2$(Hbzq)$_2$] (**2**).* To a cooled (−40 °C) dichloromethane (5 mL) solution of [*cis*-Pt(C_6F_5)$_2$(thf)$_2$] (0.075 g, 0.11 mmol) was added 2 equiv of 7,8-benzoquinoline (Hbzq) (0.040 g, 0.22 mmol). After 5 min the solvent was removed from the resulting yellow solution and the residue treated with *n*-hexane to give **2** as a yellow solid (0.040 g, 41%). ^{1}H NMR (300 MHz, $CDCl_3$, 20 °C, δ): 12.16 (d, J = 8.3, 2H, $H^{10'}$), 8.83 (d, J = 4.5, $^3J_{Pt-H} \approx 27$, 2H, $H^{2'}$), 7.98 (t, J = 7.3, 2H), 7.73 (t, J = 6.9, 2H), 7.65 (d, J = 7.7, 2H), 7.40 (m, 4H), 6.99 (d, J = 8.7, 2H), 6.44 (m, 2H). ^{19}F NMR (282.5 MHz, $CDCl_3$, δ): −40 °C, −119.4 (d, $^3J_{Pt-F}$ = 390, 2*o*-F), −119.7 (d, $^3J_{Pt-F}$ = 484, 2*o*-F), −161.6 (t, 2*p*-F), −163.3 (m, 2*m*-F), −164.2 (m, 2*m*-F); 20 °C, −119.6 (m, br, $^3J_{Pt-F} \approx 430$, 4*o*-F), −162.2 (t, 2*p*-F), −164.5 (m, 4*m*-F). IR (cm^{-1}): $\nu_{x\text{-sens}}$(C_6F_5) 795 (m), 806 (m). MS ES(−): *m*/*z* (%) 707 [Pt(bzq)(C_6F_5)$_2$]$^-$ (100). Anal. Calcd (%) for $C_{38}F_{10}H_{18}N_2Pt$: C, 51.42; H, 2.04; N, 3.16. Found: C, 51.07; H, 2.06; N, 3.09%.

*Preparation of [Pt(bzq)(C_6F_5)(Hbzq)] (**3**).* Hbzq (0.023 g, 0.13 mmol) was added to a dichloromethane (5 mL) solution of [Pt(bzq)(C_6F_5)(CH_3COCH_3)], **1**, (0.075 g, 0.13 mmol) at 0 °C. The mixture was stirred for 5 min, and the solvent was removed. Treatment of the residue with *n*-hexane yielded **3** as a yellow solid (0.070 g, 75%). ^{1}H NMR (300 MHz, $CDCl_3$, 20 °C, δ): 12.44 (d, J = 6.8, $H^{10'}$, Hbzq), 10.14 (d, J = 4.6, $H^{2'}$, Hbzq), 8.42 (d, J = 7.7, $H^{4'}$,

dx.doi.org/10.1021/ic301563u | *Inorg. Chem.* 2012, 51, 11665−11679

Hbzq), 8.22 (d, J = 8.0, H^2, bzq), 7.91 (m, 2H), 7.79 (m, 2H), 7.77−7.60 (m, 5H, with $H^{9'}$ signal at δ 7.71, and $H^{3'}$ signal at δ 7.68), 7.41 (t, J = 7.5, 1H), 7.25 (m, 1H), 7.11 (m, 2H). ^{19}F NMR (282.5 MHz, $CDCl_3$, 20 °C, δ): −116.1 (d, $^3J_{Pt-F}$ = 469, o-F), −120.2 (d, $^3J_{Pt-F}$ = 489, o-F), −163.5 (t, p-F), −164.5 (m, m-F), −165.0 (m, m-F). $^{13}C\{^1H\}$ NMR (100.6 MHz, $CDCl_3$, −40 °C, δ): 154.9 (s, $C^{2'}$, Hbzq), 153.9 (s), 153.8 (s), 149.0 (dm, C_6F_5), 146.1 (s), 145.5 (s), 142.0 (s, C^{10}, bzq), 139.2 (s, $C^{4'}$, Hbzq), 137.7 (s, C^2, bzq), 136.8 (dm, C_6F_5), 134.9 (s), 134.2 (s), 134.1 (s), 134.0 (s), 130.1(s), 129.9 (s), 129.8 (s), 129.7 (s), 128.6 (s), 128.5 (s), 127.7 (s), 127.2 (s, $C^{10'}$, Hbzq), 126.8 (s), 125.9 (s), 123.4 (s), 122.4 (s), 122.3 (s, $C^{3'}$, Hbzq), 121.8 (s, bzq). IR (cm^{-1}): $\nu_{x\text{-sens}}(C_6F_5)$ 797 (m). MS ES(−): m/z (%) 540 [M − (Hbzq)]$^-$ (19). Anal. Calcd (%) for $C_{32}F_5H_{17}N_2Pt$: C, 53.41; H, 2.38; N, 3.89. Found: C, 53.63; H, 2.54; N, 3.52%.

Synthesis of [Pt(bzq)(C_6F_5)(HC≡CR)] (R = Ph 4, ^{t}Bu 5, Fc 6). To a solution of [Pt(bzq)(C_6F_5)(CH_3COCH_3)], **1**, (0.130 g, 0.217 mmol) in CH_2Cl_2 (∼ 20 mL) was added the corresponding alkyne (0.217 mmol) and the mixture stirred for 30 min. Then the solvent was removed under vacuum and the residue treated with Et_2O (5 mL) to give the products as yellow (**4** and **5**) or orange (**6**) solids.

*Data for [Pt(bzq)(C_6F_5)(HC≡CPh)] (**4**).* Yield (0.098 g, 70%). ^{1}H NMR ($CDCl_3$, 20 °C, δ): 8.66 (d, $^3J_{H-H}$ = 4.9 Hz, 1H, bzq), 8.32 (d, $^3J_{H-H}$ = 7.9 Hz, 1H, bzq), 7.91 (d, $^3J_{H-H}$ = 7.4 Hz, 1H, bzq), 7.81 (d, $^3J_{H-H}$ = 8.7 Hz, 1H, bzq), 7.69 (d, $^3J_{H-H}$ = 7.8 Hz, 1H, bzq), 7.58 (d, $^3J_{H-H}$ = 8.7 Hz, 1H, bzq), 7.50 (t, $^3J_{H-H}$ = 9.1 Hz, 1H, bzq), 7.48 (t, $^3J_{H-H}$ = 7.6 Hz, 1H, bzq), 7.40−7.22 (m, Ph), 7.15 (s, Ph), 7.13 (s, Ph), 4.91 (s, J_{Pt-H} = 46 Hz, 1H, HC≡CPh). ^{19}F NMR (282.4 MHz, $CDCl_3$, 20 °C, δ): −118.7 (d, $J_{Pt\text{-}oF}$ = 450 Hz, 2o-F), −162.3 (t, 1p-F), −164.0 (m, 2m-F). IR(cm^{-1}): ν(≡C−H) 3233 (s), ν(C≡C) 1985 (m), $\nu(C_6F_5)_{X\text{-sens}}$ 802 (m). MALDI-TOF (−): m/z 641 [M − H]$^-$ (28%). Anal. Calcd (%) for $C_{27}H_{14}F_5NPt$: C, 50.47; H, 2.20; N, 2.18. Found: C, 50.06; H, 1.88; N, 1.98%.

*Data for [Pt(bzq)(C_6F_5)(HC≡C^{t}Bu)] (**5**).* Yield (0.058 g, 43%). ^{1}H NMR (400 MHz, $CDCl_3$, 20 °C, δ): 8.81 (d, J = 4.4, $^3J_{Pt-H}$ = 45, H^2, bzq), 8.39 (d, J = 7.6, H^4, bzq), 7.83 (d, J = 8.4, H^6, bzq), 7.70 (d, $J \approx$ 8, H^7, bzq), 7.61 (m, H^3/H^5, bzq), 7.51 (t, J = 7.2, H^8, bzq), 7.18 (d, J = 7.2, $^3J_{Pt-H}$ = 82, H^9, bzq), 4.15 (s, J_{Pt-H} = 50, 1H, HC≡C^{t}Bu), 1.33 (s, 9H, ^{t}Bu). ^{19}F NMR (282.4 MHz, $CDCl_3$, 20 °C, δ): −115.2 (d, $J_{Pt\text{-}oF}$ = 448, o-F), −120.8 (d, $J_{Pt\text{-}oF}$ = 445, o-F), −162.5 (t, 1p-F), −164.0 (m, m-F), −164.6 (m, m-F). $^{13}C\{^1H\}$ NMR (100.62 MHz, $CDCl_3$, 20 °C, δ): 143.7 (s, bzq), 137.7 (s, bzq), 133.7 (s, bzq), 129.2 (s, bzq), 124.4 (s, bzq), 122.6 (s, bzq), 120.9 (s, bzq), 120.8 (s, bzq), 95.1 (s, C≡CR), 65.7 (s, H-C≡), 30.5 (s, $C(CH_3)_3$), 30.2 (s, $C(CH_3)_3$). IR(cm^{-1}): ν(≡C−H) 3253, 3245 (s); ν(C≡C) 1974 (m), $\nu(C_6F_5)_{X\text{-sens}}$ 802 (s). MALDI-TOF (+): 620 [M]$^+$ (8%). Anal. Calcd (%) for $C_{25}H_{18}F_5NPt$: C, 48.24; H, 2.91; N, 2.25. Found: C, 47.98; H, 2.83; N, 2.01%.

*Data for [Pt(bzq)(C_6F_5)(HC≡CFc)] (**6**).* Yield (0.105 g, 65%). ^{1}H NMR (400 MHz, $CDCl_3$, 20 °C, δ): 8.67 (d, J = 5.2, $^3J_{Pt-H} \approx$ 25, H^2, bzq), 8.33 (d, $J \approx$ 8, H^4, bzq), 7.81 (d, J = 8.8, H^6, bzq), 7.68 (d, $J \approx$ 7.6, H^7, bzq), 7.58 (d, J = 8.4, H^5, bzq), 7.51 (m, H^3/H^8, bzq), 7.15 (d, J = 7.2, $^3J_{Pt-H}$ = 68, H^9, bzq), 4.77 (s, 2H, C_5H_4, Fc), 4.47 (s, J_{Pt-H} = 48, 1H, HC≡CFc), 4.28 (s, 2H, C_5H_4, Fc), 4.08 (s, 5H, Cp, Fc). ^{19}F NMR (282.4 MHz, $CDCl_3$, 20 °C, δ): −117.9 (d, $J_{Pt\text{-}oF}$ = 462, 2o-F), −162.2 (t, 1p-F), −164.0 (m, 2m-F). IR(cm^{-1}): ν(≡C−H) 3215 (s), ν(C≡C) 1996 (m), $\nu(C_6F_5)_{X\text{-sens}}$ 809 (m). MALDI-TOF (+): 750 [M]$^+$ (8%). Anal. Calcd (%) for $C_{31}H_{18}F_5FeNPt$: C, 49.62; H, 2.42; N, 1.87. Found: C, 49.48; H, 2.36; N, 1.53%.

Synthesis of [Pt(bzq)(C_6F_5)(PhC≡CPh)] (7). Compound **7** was prepared as a yellow solid following the same procedure as for **4** using [Pt(bzq)(C_6F_5)(CH_3COCH_3)] (0.150 g, 0.250 mmol) and PhC≡CPh (0.046 g, 0.250 mmol) (0.163 g, 90%). ^{1}H NMR (400 MHz, $CDCl_3$, 20 °C, δ): 8.58 (d, J = 4.4, $^3J_{Pt-H}$ = 26, H^2, bzq), 8.34 (d, J = 8.8, H^4, bzq), 7.95 (d, J = 6.8, 4H, o-Ph), 7.87 (d, J = 8.4, H^6, bzq), 7.80 (d, $J \approx$ 8, H^7, bzq), 7.64 (d, $J \approx$ 6, H^5, bzq), 7.58 (m, H^8, bzq), 7.42 (m, H^3, bzq), 7.37−7.30 (6H, m,p-Ph), 7.19 (d, J = 7.6, $^3J_{Pt-H}$ = 66, H^9, bzq). ^{19}F NMR (282.4 MHz, $CDCl_3$, 20 °C, δ): −117.0 (dm, $J_{Pt\text{-}oF}$ = 426, 2o-F), −162.7 (t, 1p-F), −164.4 (m, 2m-F). IR(cm^{-1}): ν(C≡C) 2017 (m), $\nu(C_6F_5)_{X\text{-sens}}$ 802 (m). MALDI-TOF (+): 718 [M]$^+$ (53%). Anal. Calcd (%) for $C_{33}H_{18}F_5NPt$: C, 55.16; H, 2.52; N, 1.95. Found: C, 54.96; H, 2.33; N, 2.01%.

Computational Details for Theoretical Calculations. DFT calculations were performed on complexes **3**, **4**, **4′**, **6**, and the dimer $\mathbf{3}_2$ with Gaussian 03 (revision E.01).[40] Geometries in the S^0 ground state were optimized using the B3LYP method for all complexes and in the T^1 excited state for complexes **3**, $\mathbf{3}_2$, and **4** using the unrestricted U-B3LYP (T^1) Becke's three-parameter functional combined with Lee−Yang−Parr's correlation functional.[41] No negative frequency was found in the vibrational frequency analysis. $\mathbf{3}_2$ was optimized starting from a dimer obtained by the $\pi\cdots\pi$ interactions in the X-ray diffraction study of complex **3**. The basis set used for the platinum centers was the LanL2DZ effective core potential[42] and 6-31G(d,p) for the ligand atoms. The solvent effect of the tetrahydrofuran or dichloromethane in the TD-DFT calculations was taken in consideration by the polarizable continuum model (PCM).[43]

X-ray Crystallography. Details of the structural analyses for complex **3** and **8** are summarized in Table 4. Pale yellow (**3**) or orange (**8**) crystals were obtained by slow diffusion at −30 °C of n-hexane into solutions of the complexes in CH_2Cl_2. X-ray intensity data were collected with a NONIUS-κCCD area-detector diffractometer, using graphite-monochromated Mo Kα radiation, and the images were processed using the DENZO and SCALEPACK suite of programs,[44] carrying out the absorption correction at this point for complex **3**. For complex **8**, the absorption correction was performed using SORTAV.[45] The structures were solved by Direct and Patterson Methods using SIR2004[46] (**3**) or DIRDIF96[47] (**8**), and refined by full-matrix least-squares on F^2 with SHELXL-97.[48] All non-hydrogen atoms were assigned anisotropic displacement parameters. All the hydrogen atoms were constrained to idealized geometries fixing isotropic displacement parameters 1.2 times the U_{iso} value of their attached carbon. For both structures, the correct assignment of the position of the C and N atoms bonded to platinum in the benzoquinolate ligand was confirmed by examination of the

Table 4. Crystallographic Data for $\mathbf{3}\cdot 0.25CH_2Cl_2$ and $\mathbf{8}\cdot 2.5CH_2Cl_2\cdot H_2O$

empirical formula	$C_{32.5}Cl_{0.5}H_{17.5}F_5N_2Pt$	$C_{64.5}Cl_5H_{41}F_{10}Fe_2N_2OPt_2$
F_w	740.80	1729.17
T (K)	173(1)	123(1)
cryst syst; space group	triclinic; $P\bar{1}$	triclinic; $P\bar{1}$
a (Å); α (deg)	8.1679(7); 71.521(4)	13.4380(8); 108.519(3)
b (Å); β (deg)	12.3058(9); 84.253(5)	14.3390(9); 91.022(4)
c (Å); γ (deg)	14.3251(7); 84.989(3)	14.4630(9); 93.348(3)
V (Å^3); Z	1356.39(17); 2	2636.1(3); 2
D_{calcd} (Mg/m^3)	1.814	2.178
abs coeff (mm^{-1})	5.281	5.908
F(000)	713	1436
cryst size (mm^2)	0.20 × 0.20 × 0.20	0.20 × 0.10 × 0.05
θ range for data collection (deg)	2.97−25.68	1.49−26.37
index ranges	$0 \le h \le 9$	$-16 \le h \le 16$
	$-14 \le k \le 15$	$-17 \le k \le 16$
	$-17 \le l \le 17$	$0 \le l \le 18$
no. data/restraints/params	5092/4/386	10 712/0/614
GOF on F^2[a]	1.094	1.046
final R indexes [$I > 2\sigma(I)$][a]	R1 = 0.0444, wR2 = 0.1151	R1 = 0.0511, wR2 = 0.1252
R indices (all data)[a]	R1 = 0.0476, wR2 = 0.1176	R1 = 0.0765, wR2 = 0.1330
largest diff peak and hole (e Å^{-3})	4.643 and −1.939	1.641 and −2.013

[a] $R1 = \Sigma(||F_o| - |F_c||)/\Sigma|F_o|$; $wR2 = [\Sigma w(F_o^2 - F_c^2)^2/\Sigma wF_o^2]^{1/2}$; GOF = $\{\Sigma[w(F_o^2 - F_c^2)^2]/(N_{obs} - N_{param})\}^{1/2}$; $w = [\sigma^2(F_o) + (g_1P)^2 + g_2P]^{-1}$; $P = [\max(F_o^2; 0) + 2F_c^2]/3$.

ΔMSDA values for bonds involving these atoms,[49] after refining each case in three different ways (with the identities of the C and N in one position, reversed, and with 50/50 hybrid scattering factor at each of the affected atomic sites). For complex **3**, 0.5 molecules of disordered crystallization CH_2Cl_2 were found in the unit cell, and four restraints were used in order to model them. For complex **8**, disordered crystallization molecules of CH_2Cl_2 and H_2O were also observed. Despite many attempts, we could not resolve the disorders adequately. The use of SQUEEZE[50] revealed the presence in the unit cell of one central void of 301 Å^3 containing 212 electrons, which fits well with the presence five molecules of CH_2Cl_2, and two little voids of 15 Å^3 containing one water molecule each of them (11 electrons). Therefore, we have included them in the empirical formula as crystallization solvent (**8**·2.5$CHCl_3$·H_2O). Finally, both structures show some residual peaks greater than 1 e Å^{-3} in the vicinity of the platinum atoms or the crystallization solvent, but with no chemical meaning.

■ ASSOCIATED CONTENT

Supporting Information

Additional figures and tables. Complete reference for Gaussian 03 (revision E.01). This material is available free of charge via the Internet at http://pubs.acs.org.

■ AUTHOR INFORMATION

Corresponding Author

*Fax: (+34) 941 299 621. E-mail: elena.lalinde@unirioja.es.

Notes

The authors declare no competing financial interest.

■ ACKNOWLEDGMENTS

This work was supported by the Spanish MICINN (Project CTQ2008-06669-C02-02/BQU) and by the CAR (Colabora 2009/05). S.S. thanks CSIC for a grant. The authors also thank CESGA for computer support.

■ DEDICATION

†Dedicated to Professor Juan Forniés on the occasion of his 65th birthday.

■ REFERENCES

(1) (a) Special issue: Controlling Photophysical Properties of Metal Complexes: Towards Molecular Photonics. *Coord. Chem. Rev.* Vlček, T., Guest Ed.; **2011**, *255* (21−22), 2399. (b) Guerchais, V.; Ordronneau, L.; Le Bozec, H. *Coord. Chem. Rev.* **2010**, *254*, 2553. (c) Chen, Z. N.; Zhao, N.; Fan, Y.; Ni, J. *Coord. Chem. Rev.* **2009**, *253*, 1. (d) Photofunctional Transition Metal Complexes. *Structure and Bonding*; Yam, V. W. W., Ed. Springer: Berlin, 2007; Vol. *123*. (e) Lai, S. W.; Che, C. M. *Top. Curr. Chem.* **2004**, *241*, 27. (f) Rausch, A. F.; Homeier, H. H. H.; Yersin, H. *Top. Curr. Organomet. Chem.* **2010**, *29*, 193. (g) Djurovich, P. I.; Thompson, M. E. In *Highly Efficient OLEDs with Phosphorescent Materials*; Yersin, H., Ed.; Wiley-VCH: Weinheim, 2008; p 131. (h) Xiang, H. F.; Lai, S. W.; Lai, P. T.; Che, C. M. In *Highly Efficient OLEDs with Phosphorescent Materials*; Yersin, H., Ed.; Wiley-VCH: Weinheim, Germany, 2007; p 259. (i) Evans, R. C.; Douglas, P.; Winscom, C. *Coord. Chem. Rev.* **2006**, *250*, 2093.

(2) (a) Williams, J. A. G. *Top. Curr. Chem.* **2007**, *281*, 205. (b) Williams, J. A. G. *Chem. Soc. Rev.* **2009**, *38*, 1783. (c) Williams, J. A. G.; Develay, S.; Rochester, D. L.; Murphy, L. *Coord. Chem. Rev.* **2008**, *252*, 2596. (d) Eryazici, I.; Moorefield, C. N.; Newkome, G. R. *Chem. Rev.* **2008**, *108*, 1834. (e) Berenguer, J. R.; Lalinde, E.; Moreno, M. T. *Coord. Chem. Rev.* **2010**, *254*, 832. (f) Murphy, L.; Williams, J. A. G. *Top. Organomet. Chem.* **2010**, *28*, 75. (g) Chi, Y.; Chou, P. T. *Chem. Soc. Rev.* **2010**, *39*, 638. (h) Wong, K. M. C.; Yam, V. W. W. *Coord. Chem. Rev.* **2007**, *251*, 2477. (i) Wong, W. Y. *Dalton Trans.* **2007**, 4495. (j) McGuire, R., Jr.; McGuire, M. C.; McMillin, D. R. *Coord. Chem. Rev.* **2010**, *254*, 2574. (k) Díez, A.; Lalinde, E.; Moreno, M. T. *Coord. Chem. Rev.* **2011**, *255*, 2426. (l) Wong, K. M. C.; Yam, V. W. W. *Acc. Chem. Res.* **2011**, *44*, 424. (m) Zhou, K. J.; Wong, W. Y. *Chem. Soc. Rev.* **2011**, *40*, 2541. (n) Cummings, S. D. *Coord. Chem. Rev.* **2009**, *253*, 449.

(3) (a) Yang, C.; Zhang, X.; You, H.; Zhu, L.; Chen, L.; Zhu, L.; Tao, Y.; Ma, D.; Shuai, Z.; Quin, J. *Adv. Funct. Mater.* **2007**, *17*, 651. (b) Cocchi, M.; Virgili, D.; Fattori, V.; Rochester, D. L.; Williams, J. A. G. *Adv. Funct. Mater.* **2007**, *17*, 285. (c) Chen, C. H.; Wu, F. L.; Tsai, Y. Y.; Cheng, C. H. *Adv. Funct. Mater.* **2011**, *21*, 3150. (d) Yang, X.; Wang, Z.; Madakuni, S.; Li, J.; Jabbour, G. E. *Adv. Mater.* **2008**, *20*, 2405. (e) Kui, S. C. F.; Hung, F. F.; Lai, S. L.; Yuen, M. Y.; Kwok, C. C.; Low, K. H.; Chui, S. S. Y.; Che, C. M. *Chem.—Eur. J.* **2012**, *18*, 96. (f) Ma, B.; Djurovich, P. I.; Garon, S.; Allyne, B.; Thompson, M. E. *Adv. Funct. Mater.* **2006**, *16*, 2438.

(4) (a) Koo, C. K.; So, L. K. Y.; Wong, K. L.; Ho, Y. M.; Lam, Y. W.; Lam, M. H. W.; Cheah, K. W.; Cheng, C. C. W.; Kwok, W. M. *Chem.—Eur. J.* **2010**, *16*, 3942. (b) Yam, V. W. W.; Tang, R. P. L.; Wong, K. M. C.; Lu, X. X.; Cheung, K. K.; Zhu, N. *Chem.—Eur. J.* **2002**, *8*, 4066. (c) Ma, D. L.; Che, C. M.; Yan, S. C. *J. Am. Chem. Soc.* **2009**, *131*, 1835. (d) Wu, P.; Wong, E. L. M.; Ma, D. L.; Tong, G. S. M.; Ng, K. M.; Che, C. M. *Chem.—Eur. J.* **2009**, *15*, 3652. (e) Lusby, P. J.; Müller, P.; Pine, S. J.; Slawin, A. M. Z. *J. Am. Chem. Soc.* **2009**, *131*, 16398. (f) Zhao, Q.; Li, F. Y.; Huang, C. H. *Chem. Soc. Rev.* **2010**, *39*, 3007. (g) Zhao, Q.; Li, F. Y.; Huang, C. H. *Chem. Soc. Rev.* **2011**, *40*, 2508.

(5) (a) Shavaleev, N. M.; Adams, H.; Best, J.; Edge, R.; Navaratnam, S.; Weinstein, J. *Inorg. Chem.* **2006**, *45*, 9410. (b) Zhang, J.; Du, P.; Schneider, J.; Jarosz, P.; Eisenberg, R. *J. Am. Chem. Soc.* **2007**, *129*, 7726.

(6) (a) Hissler, M.; McGarrah, J. E.; Connick, W. B.; Geiger, D. K.; Cummings, S. D.; Eisenberg, R. *Coord. Chem. Rev.* **2000**, *208*, 115. (b) Tong, G. S. M.; Che, C. M. *Chem.—Eur. J.* **2009**, *15*, 7225.

(7) (a) Brooks, J.; Babayan, Y.; Lamanski, S.; Djurovich, P. I.; Tsyba, I.; Bau, R.; Thompson, M. E. *Inorg. Chem.* **2002**, *41*, 3055. (b) Ghedini, M.; Pugliese, T.; La Deda, M.; Goldbert, N.; Aiello, I.; Amati, M.; Belviso, S.; Leli, F.; Accorsi, G.; Barigelletti, F. *Dalton Trans.* **2008**, 4303. (c) Mou, X.; Wu, Y.; Liu, S.; Shi, M.; Liu, X.; Wang, C.; Sun, S.; Zhao, Q.; Zhou, X.; Huang, W. *J. Mater. Chem.* **2011**, *21*, 13951. (d) Wu, W.; Guo, H.; Wu, W.; Ji, S.; Zhao, J. *Inorg. Chem.* **2011**, *50*, 11446.

(8) (a) Fernández, S.; Forniés, J.; Gil, B.; Gómez, J.; Lalinde, E. *Dalton Trans.* **2003**, 822. (b) Díez, A.; Forniés, J.; García, A.; Lalinde, E.; Moreno, M. T. *Inorg. Chem.* **2005**, *44*, 2443. (c) Díez, A.; Forniés, J.; Fuertes, S.; Lalinde, E.; Larraz, C.; López, J. A.; Martín, A.; Moreno, M. T.; Sicilia, V. *Organometallics* **2009**, *28*, 1705. (d) Forniés, J.; Fuertes, S.; López, J. A.; Martín, A.; Sicilia, V. *Inorg. Chem.* **2008**, *47*, 7166. (e) Díez, A.; Forniés, J.; Larraz, C.; Lalinde, E.; López, J. A.; Martín, A.; Moreno, M. T.; Sicilia, V. *Inorg. Chem.* **2010**, *49*, 3239. (f) Rausch, A. F.; Monkowins, U. V.; Zabel, M.; Yersin, H. *Inorg. Chem.* **2010**, *49*, 7818. (g) Liu, J.; Sun, R. W. Y.; Leung, C. H.; Lok, C. N.; Che, C. M. *Chem. Commun.* **2012**, *48*, 230. (h) Zheng, G. Y.; Rillema, D. P.; DePriest, J.; Woods, C. *Inorg. Chem.* **1998**, *37*, 3588.

(9) (a) Yagyu, T.; Ohashi, J. I.; Maeda, M. *Organometallics* **2007**, *26*, 2383. (b) Calvet, T.; Crespo, M.; Font-Bardia, M.; Gómez, K.; González, G.; Martínez, M. *Organometallics* **2009**, *28*, 5096. (c) Jamali, S.; Nabavizadeh, S. M.; Rashidi, M. *Inorg. Chem.* **2008**, *47*, 5441. (d) Zucca, A.; Cinellu, M. A.; Minguetti, G.; Stoccoro, S.; Monassero, M. *Eur. J. Inorg. Chem.* **2004**, 4484. (e) Minguetti, G.; Doppin, A.; Zucca, A.; Stoccoro, S.; Cinellu, M. A.; Manassero, M.; Sansoni, M. *Chem. Heterocycl. Cmpd.* **1999**, *35*, 992. (f) Martín, R.; Crespo, M.; Font-Bardia, M.; Calvet, T. *Organometallics* **2009**, *28*, 587. (g) Crespo, M.; Font-Bardia, M.; Calvet, T. *Dalton Trans.* **2011**, *40*, 9431. (h) Zhao, S. B.; Wang, R. Y.; Wang, S. *J. Am. Chem. Soc.* **2007**, *129*, 3092. (i) Nabavizadeh, S. M.; Haghighi, M. G.; Esmaeilbeig, A. R.; Raoof, F.; Mandegani, Z.; Jamali, S.; Rashidi, M.; Puddephatt, R. J. *Organometallics* **2010**, *29*, 4893. (j) Haghighi, M. G.; Rashidi, M.; Nabavizadeh, S. M.; Jamali, S.; Puddephatt, R. J. *Dalton Trans.* **2010**, *39*, 11396. (k) Rao, Y. L.; Wang, S. *Inorg. Chem.* **2009**, *48*, 7698. (l) Nabavizadeh, S. M.; Amini, H.; Shahsavari, H. R.; Namdar, M.;

Rashidi, M.; Kia, R.; Hemmateenjad, B.; Nekoeinia, M.; Ariafard, A.; Hosseini, F. N.; Ghavari, A.; Khalafi-Nezhad, A.; Sharbati, M. T.; Panahi, F. *Organometallics* **2011**, *30*, 1466.

(10) (a) Crespo, M. *Organometallics* **2012**, *31*, 1216. (b) Canty, A. J. *Dalton Trans.* **2009**, 10409. (c) Albrecht, M.; van Koten, G. *Angew. Chem., Int. Ed.* **2001**, *40*, 3750.

(11) Forniés, J.; Ibáñez, S.; Martín, A.; Gil, B.; Lalinde, E.; Moreno, M. T. *Organometallics* **2004**, *23*, 3963.

(12) (a) Forniés, J.; Ibáñez, S.; Martín, A.; Sanz, M.; Berenguer, J. R.; Lalinde, E.; Torroba, J. *Organometallics* **2006**, *25*, 4331. (b) Forniés, J.; Ibáñez, S.; Lalinde, E.; Martín, A.; Moreno, M. T.; Tsipis, A. C. *Dalton Trans.* **2012**, 3439.

(13) (a) Steinborn, D.; Tschoerner, M.; von Zweidorf, A.; Sieler, J.; Bögel, H. *Inorg. Chim. Acta* **1995**, *234*, 47. (b) Gerisch, M.; Heinemann, F. W.; Bögel, H.; Steinborn, D. *J. Organomet. Chem.* **1997**, *548*, 247. (c) Fanizzi, F. P.; Natile, G.; Lanfranchi, M.; Tiripicchio, A.; Pacchioni, G. *Inorg. Chim. Acta* **1998**, *275*−*276*, 500. (d) Engelman, K. L.; White, P. S.; Templeton, J. L. *Inorg. Chim. Acta* **2009**, *362*, 4461. (e) Clark, H. C.; Manzer, L. E. *Inorg. Chem.* **1974**, *13*, 1291.

(14) (a) Forniés, J.; Lalinde, E. In *Comprehensive Organometallic Chemistry III*; Crabtree, R. H., Mingos, D. M. P., Eds.; Elsevier: Oxford, 2007; Vol *8*. p 611. (b) Young, G. B. In *Comprehensive Organometallic Chemistry*; Abel, E. W., Stone, F. G. A., Wilkinson, G., Elsevier: Oxford, 1995; Vol. *9*, p 553. (c) Belluco, U.; Bertani, R.; Michelin, R. A.; Mozzon, M. *J. Organomet. Chem.* **2000**, *600*, 37.

(15) (a) Albrecht, M. *Chem. Rev.* **2010**, *110*, 576 and references therein. (b) Omay, I. *Coord. Chem. Rev.* **2004**, *248*, 995. (c) Steenwinkel, P.; Gossage, R. A.; van Koten, G. *Chem.—Eur. J.* **1998**, *4*, 759. (d) Ryabov, A. D. *Chem. Rev.* **1990**, *90*, 403. (e) Dupont, J.; Consorti, C. S.; Spencer, J. *Chem. Rev.* **2005**, *105*, 2527. (f) Niu, J. L.; Hao, X. Q.; Gong, J. F.; Song, M. P. *Dalton Trans.* **2011**, *40*, 5135. (g) Canty, A. J. *Acc. Chem. Res.* **1992**, *25*, 83. (h) Rendina, L. M.; Puddephatt, R. J. *Chem. Rev.* **1997**, *97*, 1735.

(16) Cope, A. C.; Siekman, R. W. *J. Am. Chem. Soc.* **1965**, *87*, 3272.

(17) (a) Zucca, A.; Cordeschi, D.; Stoccoro, S.; Cinellu, M. A.; Minguetti, G.; Chelucci, G.; Manassero, M. *Organometallics* **2011**, *30*, 3064. (b) Zucca, A.; Petretto, G. L.; Cabras, M. L.; Stoccoro, S.; Cinellu, M. A.; Manassero, M.; Minghetti, G. *J. Organomet. Chem.* **2009**, *694*, 3753. (c) Zucca, A.; Petretto, G. L.; Stoccoro, S.; Cinellu, M. A.; Manassero, M.; Manassero, C.; Minguetti, G. *Organometallics* **2009**, *28*, 2150. (d) Minguetti, G.; Stoccoro, S.; Cinellu, M. A.; Petretto, G. L.; Zucca, A. *Organometallics* **2008**, *27*, 3415. (e) Zucca, A.; Petretto, G. L.; Stoccoro, S.; Cinellu, M. A.; Minghetti, G.; Manassero, M.; Manassero, C.; Male, L.; Albinati, A. *Organometallics* **2006**, *25*, 2253. (f) Crosby, S. H.; Clarkson, G. J.; Rourke, J. P. *Organometallics* **2011**, *30*, 3603.

(18) Forniés, J.; Menjón, B.; Gómez, N.; Tomás, M. *Organometallics* **1992**, *11*, 1187.

(19) (a) Vicente, J.; Arcas, A.; Bautista, D.; Jones, P. G. *Organometallics* **1997**, *16*, 2127. (b) Vicente, J.; Arcas, A.; Galvez-López, M. D.; Jones, P. G. *Organometallics* **2006**, *25*, 4247. (c) Casas, J. M.; Forniés, J.; Fuertes, S.; Martín, A.; Sicilia, V. *Organometallics* **2007**, *26*, 1674.

(20) Alsters, P. L.; Engel, P. F.; Hogerheide, M. P.; Copijn, M.; Spek, A. L.; van Koten, G. *Organometallics* **1993**, *12*, 1831.

(21) As previously suggested, the C−H bond activation could take place through an oxidative addition leading to a pentacoordinated Pt(IV) hydride intermediate. The final cyclometalated **1** will be formed by a subsequent fast reductive elimination of the hydride and the C_6F_5 group and coordination of the acetone solvent. Unfortunately, we have not detected any intermediate hydride complex, and therefore, its implication in the pathway leading to **1** is only speculative.

(22) Albinati, A.; Pregosin, P. S.; Wombacher, F. *Inorg. Chem.* **1990**, *29*, 1812.

(23) (a) Chatterjee, S.; Krause, J. A.; Madduma-Liyanage, K.; Connick, W. B. *Inorg. Chem.* **2012**, *51*, 4572. (b) Casas, J. M.; Falvello, L. R.; Forniés, J.; Martín, A. *Inorg. Chem.* **1996**, *35*, 6009. (c) Casas, J. M.; Falvello, L. R.; Forniés, J.; Martín, A. *J. Chem. Soc., Dalton Trans.* **1997**, 1559.

(24) (a) König, A.; Bette, M.; Wagner, C.; Linder, R.; Steinborn, D. *Organometallics* **2011**, *30*, 5919. (b) Usón, R.; Forniés, J.; Tomás, M.; Menjón, B.; Fortuño, C.; Welch, A. J.; Smith, D. E. *J. Chem. Soc., Dalton Trans.* **1993**, 275. (c) Usón, R.; Forniés, J.; Tomás, M.; Menjón, B.; Welch, A. J. *J. Organomet. Chem.* **1986**, *304*, C24. (d) Tanabe, M.; Osakada, K. *Chem.—Eur. J.* **2004**, *10*, 416. (e) Huber, C.; Bangerter, F.; Caseri, W. R.; Weder, C. *J. Am. Chem. Soc.* **2001**, *123*, 3857.

(25) (a) Yam, V. W. W.; Lo, K. K. W.; Wong, K. M. C. *J. Organomet. Chem.* **1999**, *578*, 3. (b) Forniés, J.; Lalinde, E. *J. Chem. Soc., Dalton Trans.* **1996**, 2587. (c) Wong, K. M. C.; Lam, W. H.; Zhou, Z. Y.; Yam, V. W. W. *Chem.—Eur. J.* **2008**, *14*, 10928.

(26) Marinelli, G.; Streib, W. E.; Huffman, J. C.; Gagne, M. R.; Takats, J.; Dartiguenave, M.; Chardon, C.; Jackson, S. A.; Einsteins, O. *Polyhedron* **1990**, *9*, 1867.

(27) (a) Carlisle, S.; Matta, A.; Valles, H.; Bracken, J. B.; Miranda, M.; Yoo, J.; Hahn, C. *Organometallics* **2011**, *30*, 6446 and references therein. (b) Cucciolito, M. E.; de Renzi, A.; Roviello, G.; Ruffo, F. *Organometallics* **2008**, *27*, 1351. (c) West, N. M.; White, P. S.; Templeton, J. L. *Organometallics* **2008**, *27*, 5252. (d) Sagawa, T.; Sakamoto, Y.; Tanaka, R.; Katayama, H.; Ozawa, F. *Organometallics* **2003**, *22*, 4433. (e) Lucey, D. W.; Atwood, J. D. *Organometallics* **2002**, *21*, 2481. (f) Appleton, T. G.; Clark, H. C.; Puddephatt, R. J. *Inorg. Chem.* **1972**, *11*, 2074.

(28) (a) Belluco, U.; Bertani, R.; Fornasiero, S.; Michelin, R. A.; Mozzon, M. *Inorg. Chim. Acta* **1998**, *275*−*276*, 515. (b) Belluco, U.; Bertani, R.; Michelin, R. A.; Mozzon, M.; Benetollo, F.; Bomberi, G.; Angelici, R. J. *Inorg. Chim. Acta* **1995**, *240*, 567. (c) Cucciolitto, M. E.; De Felice, V.; Orabona, I.; Ruffo, F. *J. Chem. Soc., Dalton Trans.* **1997**, 1351. (d) Clark, H. C.; Manzer, L. E. *J. Am. Chem. Soc.* **1973**, *95*, 3812.

(29) (a) Nordhoff, K.; Steinborn, D. *Organometallics* **2001**, *20*, 1408. (b) Karonik, M.; Lesage, D.; Gimbert, Y.; Nava, P.; Humbel, S.; Giordanos, L.; Buono, G.; Tabet, J. C. *Organometallics* **2011**, *30*, 4814.

(30) Belluco, U.; Bertani, R.; Meneghetti, F.; Michelin, R. A.; Mozzon, M. *J. Organomet. Chem.* **1999**, *583*, 131.

(31) Berenguer, J. R.; Forniés, J.; Lalinde, E.; Martínez, F. *Organometallics* **1995**, *14*, 2532.

(32) *Modern Acetylene Chemistry*; Stang, P. J., Diederich, F., Eds.; VCH: Weinheim, Germany, 1995.

(33) (a) Powers, D. C.; Geibel, M. A. L.; Klein, J. E. M. N.; Ritter, T. *J. Am. Chem. Soc.* **2009**, *131*, 17050. (b) Powers, D. C.; Benítez, D.; Tkatchouk, E.; Goddard, W. A., III; Ritter, T. *J. Am. Chem. Soc.* **2010**, *132*, 14092.

(34) Berenguer, J. R.; Forniés, J.; Lalinde, E.; Martínez, F.; Urriolabeitia, E.; Welch, A. J. *Dalton Trans.* **1994**, 1291.

(35) Berenguer, J. R.; Díez, A.; Lalinde, E.; Moreno, M. T.; Ruiz, S.; Sánchez, S. *Organometallics* **2011**, *30*, 5776.

(36) (a) Bhadbhade, M. M.; Das, A.; Jeffery, J. C.; McCleverty, J. A.; Navas Badiola., J. A.; Ward, M. D. *J. Chem. Soc., Dalton Trans.* **1995**, 2769. (b) Barlow, S.; Bunting, H. E.; Ringham, C.; Green, J. C.; Bublitz, G. U.; Boxer, S. G.; Perry, J. W.; Marder, S. R. *J. Am. Chem. Soc.* **1999**, 3715. (c) Díez, A.; Fernández, J.; Lalinde, E.; Moreno, M. T.; Sánchez, S. *Dalton Trans.* **2008**, 4926.

(37) (a) Lee, E. J.; Wrighton, M. S. *J. Am. Chem. Soc.* **1991**, *113*, 8562. (b) Fery-Forgues, S.; Delavaux-Nicot, B. *J. Photochem. Photobiol., A* **2000**, *132*, 137. (c) Fery-Forgues, S.; Delavaux-Nicot, B.; Lavabre, D.; Rurack, K. *J. Photochem. Photobiol., A* **2003**, *155*, 107.

(38) Zhao, Q.; Li, L.; Li, F.; Yu, M.; Liu, Z.; Yi, T.; Huang, C. *Chem. Commun.* **2008**, 685.

(39) Usón, R.; Forniés, J.; Tomás, M.; Menjón, B. *Organometallics* **1985**, *4*, 1912.

(40) Frisch, M. J.; et al. *Gaussian 03, Revision E.01*: Gaussian, Inc.: Wallingford, CT, 2004 (see the Supporting Information for the complete citation).

(41) (a) Becke, A. D. *Phys. Rev. A* **1988**, *38*, 3098. (b) Becke, A. D. *J. Chem. Phys.* **1993**, *98*, 5648. (c) Lee, C.; Yang, W.; Parr, R. G. *Phys. Rev. B* **1988**, *37*, 785.

(42) Wadt, W. R.; Hay, P. J. *J. Chem. Phys.* **1985**, *82*, 284.
(43) Barone, V.; Cossi, M. *J. Phys. Chem. A* **1998**, *102*, 1995.
(44) Otwinosky, Z.; Minor, W. In *Methods Enzymology*; Carter Jr., C. V., Sweet, R. M., Eds.; Academic Press:: New York, 1997; Vol. *276A*, p 307.
(45) Blessing, R. H. *Acta Crystallogr.* **1995**, *A51*, 33.
(46) Burla, M. C.; Caliandro, R.; Carrozzini, B.; Cascarano, G. L.; De Caro, L.; Giacovazzo, C.; Polidori, G.; Spagna, R. *J. Appl. Crystallogr.* **2005**, *38*, 381.
(47) Beurskens, P. T.; Beurskens, G.; Bosman, W. P.; de Gelder, R.; Garcia-Granda, S.; Gould, R. O.; Israel, R.; Smits, J. *DIRDIF96 Program System*; M. M. Crystallography Laboratory University of Nijmegen: The Netherlands, 1996.
(48) Sheldrick, G. M. *SHELX-97, A Program for the Refinement of Crystal Structures*; University of Göttingen: Göttingen, Germany, 1997.
(49) (a) Speck, A. L. *Acta Crystallogr., Sect. A.* **1990**, *46*, c34. (b) Hirshfeld, F. L. *Acta Crystalogr., Sect. A.* **1976**, *32*, 239.
(50) Spek, A. L. *SQUEEZE, Incorporated into PLATON: A Multipurpose Crystallographic Tool*; University of Utrecht: Utrecht, The Netherlands, 2005.